DigitalWorld 2017

ACHI 2017 / eKNOW 2017 / eLmL 2017/ ICDS 2017 / GEOProcessing 2017 / ALLSENSORS 2017 / eTELEMED 2016 / SMART ACCESSIBILITY 2017 / MATH 2017 / EVIDEM 2017

March 19 - 23, 2017 - Nice, France

Embrapa Instrumentation

CT Scanner and Applications in Soil Science: Fundamentals, X-ray Sensors and Detectors, Architectures and Algorithms for Image Reconstruction and Scientific Visualization

Paulo E. Cruvinel, Ph.D.
paulo.cruvinel@embrapa.br

What is X-Ray Computed Tomography (CT)?

- Considering a short definition CT, which is also referred to as CAT, for Computed Axial Tomography, utilizes X-ray technology and sophisticated instrumentation, sensors & computers to create images of cross-sectional “slices” through a body under analysis.

- CT exams and CAT scanning provide a quick overview of morphologies and its quantification (also those related to pathologies) and enable rapid analysis and plans for prognostics and support for decision maker.

- Tomography is a term that refers to the ability to view an anatomic section or slice through the body.

- Anatomic cross sections are most commonly refers to transverse axial tomography

What is displayed in CT images?

$$CT\# = \frac{\mu_T - \mu_{water}}{\mu_{water}} \times 1000\text{HU}$$

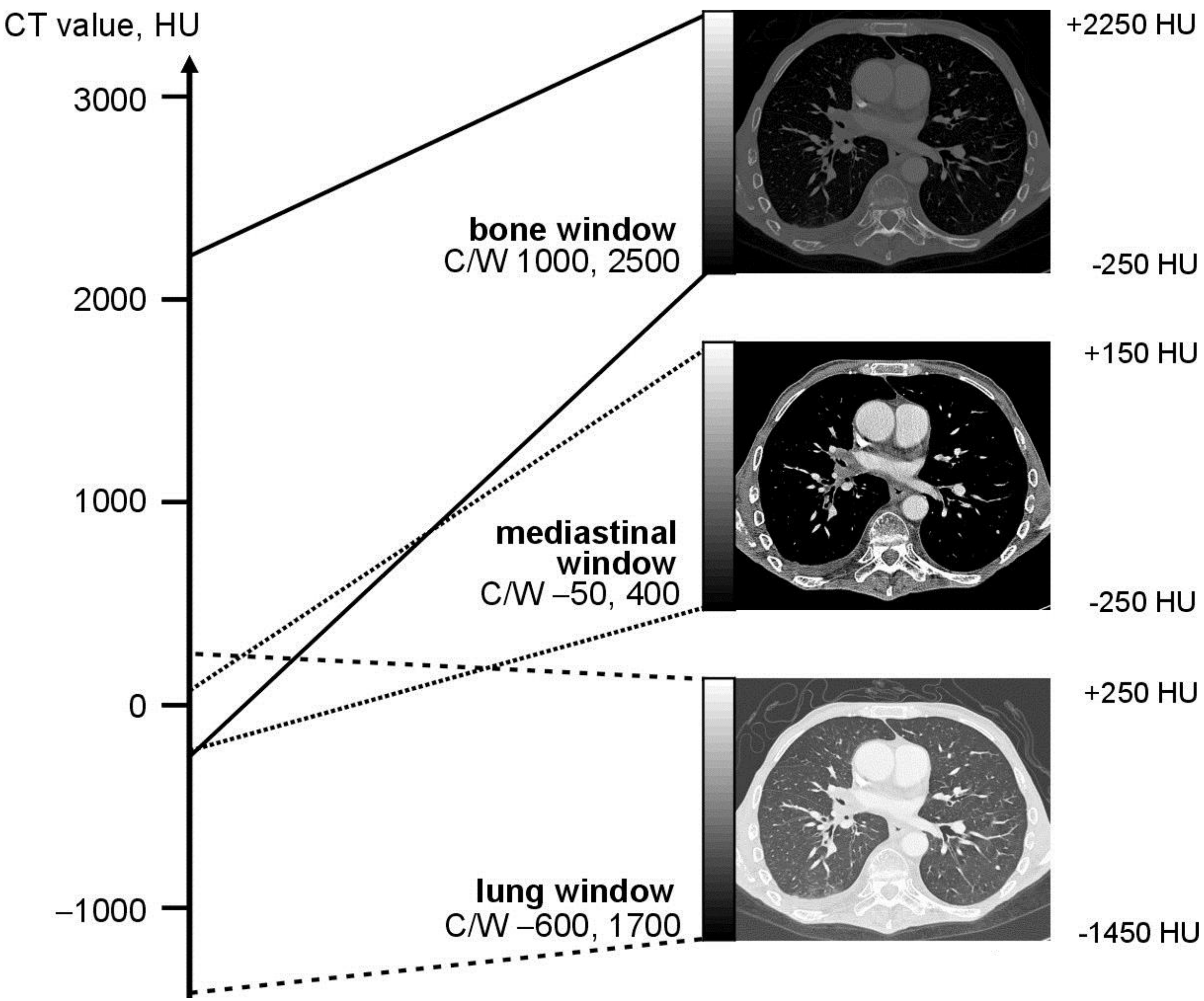

Water: 0HU

Air: -1000HU

Some Words About the History of X-Ray Computed Tomography (CT)

"*We could limit the story of the beginnings of computed tomography to mentioning Cormack and Hounsfield, the authors of this groundbreaking invention, and to placing their achievements on a timeline, from Cormack's theoretical idea in the late 1950s to Hounsfield's development of a practical device in the late 1970s*"

Allan MacLeod Cormack

- Cormack developed the mathematical technique to reconstruct images using the backprojection method based on a finite number of projections [Cormack, 1963];
- Hounsfield developed the first commercial tomograph [Housfield, 1973].

Godfrey Newbold Hounsfield

Cormack AM (1973) Reconstruction of densities from their projections, with applications in radiological physics. Phys Med Biol 18(2):195–207.
Hounsfield GN (1973) Computerized transverse axial scanning (tomography)—part 1. Description of the system. Br J Radiol 46:1016–1022.

- Radon (1887- 1956) presents the mathematical principles of a body reconstruction from their projections considering a space with order equal to n [Radon, 1917];

In mathematics, the **Radon transform** is the integral transform which takes a function *f* defined on the plane to a function *Rf* defined on the space of lines in the plane, whose value at a particular line is equal to the line integral of the function over that line (introduced in 1917 and also provided a formula for the inverse transform).

Johann Karl August Radon

Radon, Johann (1917), "Über die Bestimmung von Funktionen durch ihre Integralwerte längs gewisser Mannigfaltigkeiten", Berichte über die Verhandlungen der Königlich-Sächsischen Akademie der Wissenschaften zu Leipzig, Mathematisch-Physische Klasse [Reports on the proceedings of the Royal Saxonian Academy of Sciences at Leipzig, mathematical and physical section], Leipzig: Teubner (69): 262–277; Translation: Radon, J.; Parks, P.C. (translator) (1986), "On the determination of functions from their integral values along certain manifolds", IEEE Transactions on Medical Imaging, ***5*** *(4): 170–176.*

- CT uses electromagnetic wave, i.e., X-radiation.

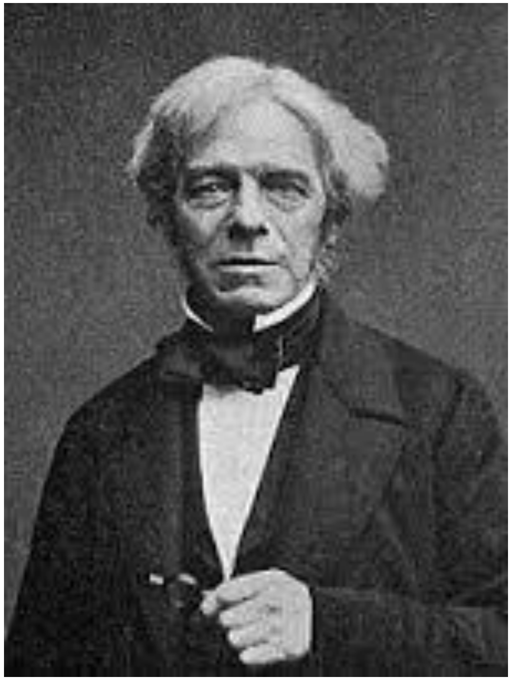

Michael Faraday (1791–1867) observed the phenomenon of electromagnetism and in 1831 formulated the laws of electromagnetic induction.

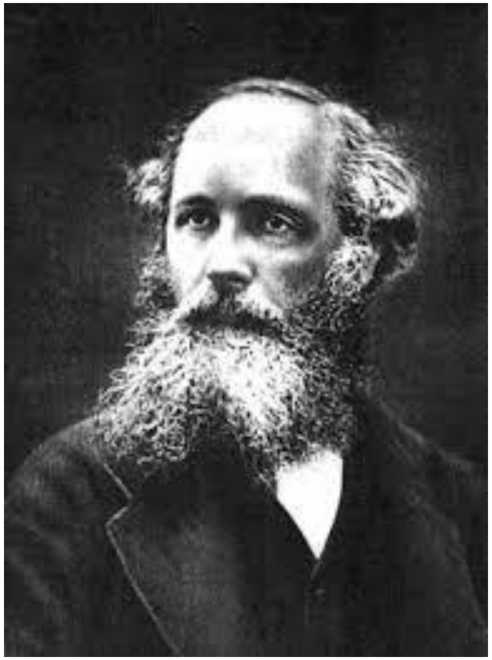

Twenty-nine years later, in 1860, James Clark Maxwell (1831-1879), formulates the Maxwell's equations, comprehensively expressed the ideas of electricity and magnetism, which led to the development of the later technologies of radio and television and of course, radiology.

- Wilhelm Röntgen (1845-1923) was the first to systematically study the X-rays in 1895.

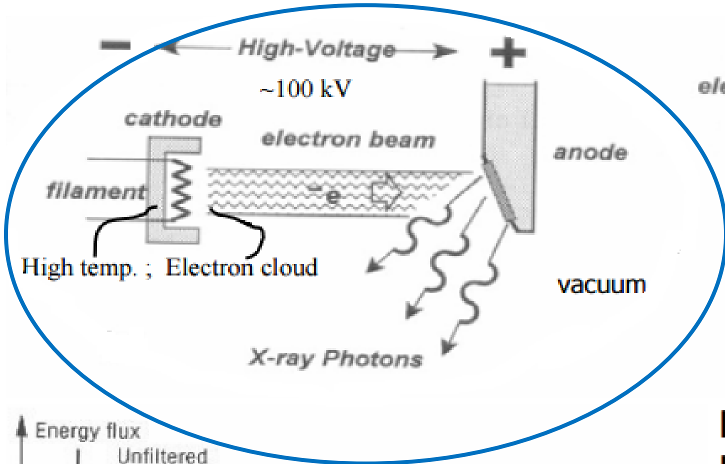

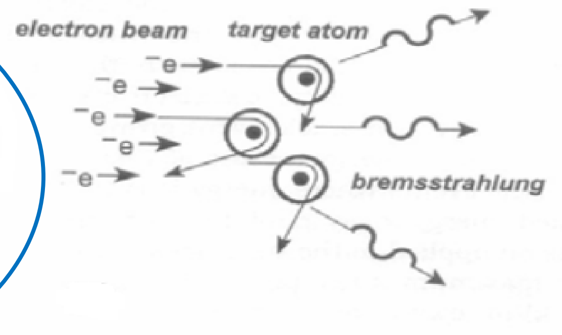

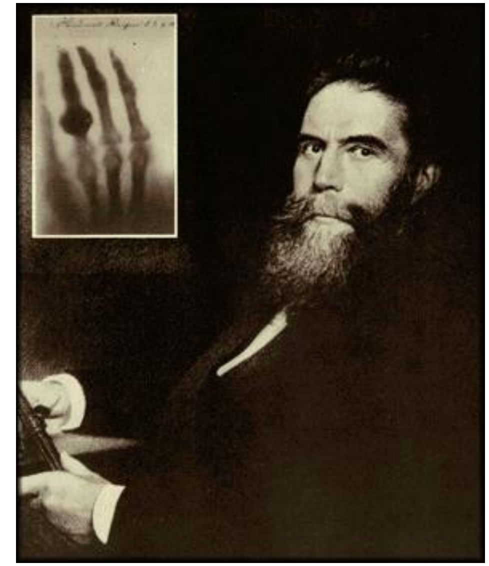

Wilhelm C. Röntgen

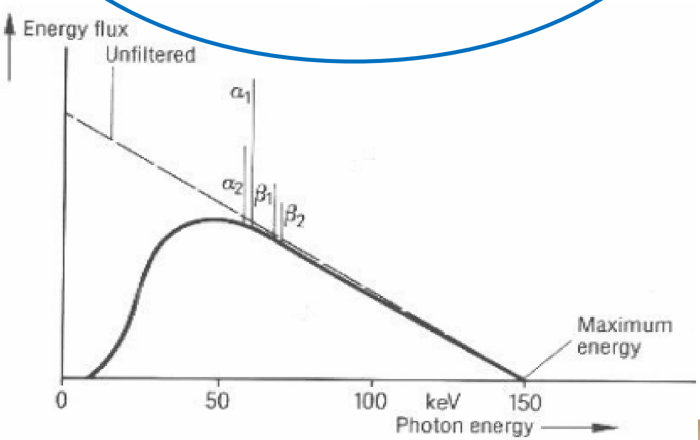

Production of X-rays and Bremsstrahlung (stopping radiation) – thermal electron emission in vacuum (10^{-6} mbar) and target bombardment

White X-ray spectrum (gamma quanta with all energies) and its final view (after tube filtration)

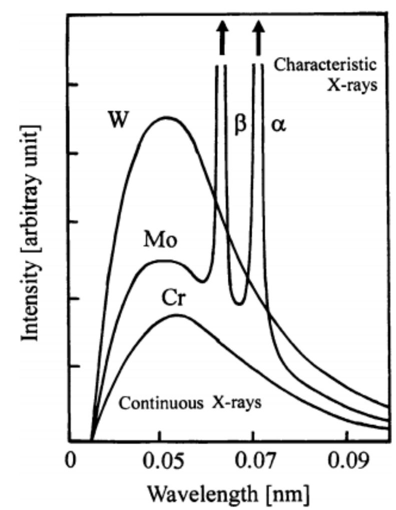

Stationary anode

Rotating anode

Röntgen CW (1895) Uber eine neue Art von Strahlen. Vorläufige Mitteilung.

The Nobel Prize in Physiology or Medicine 1979

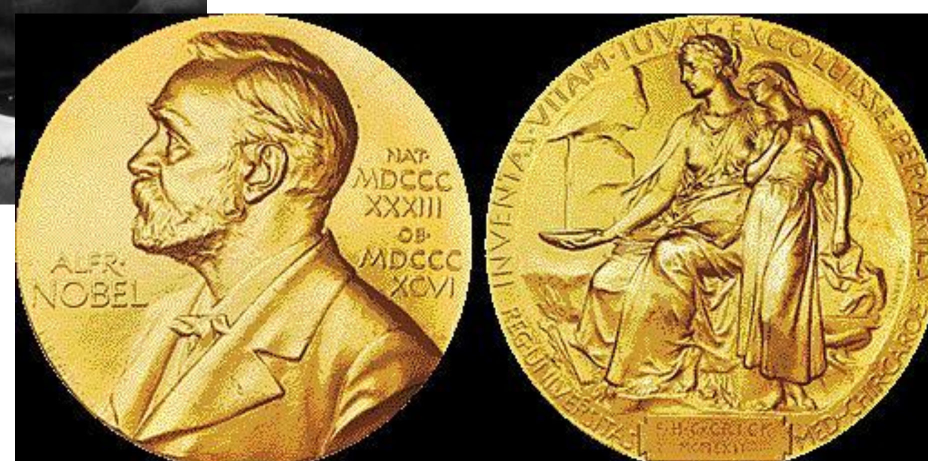

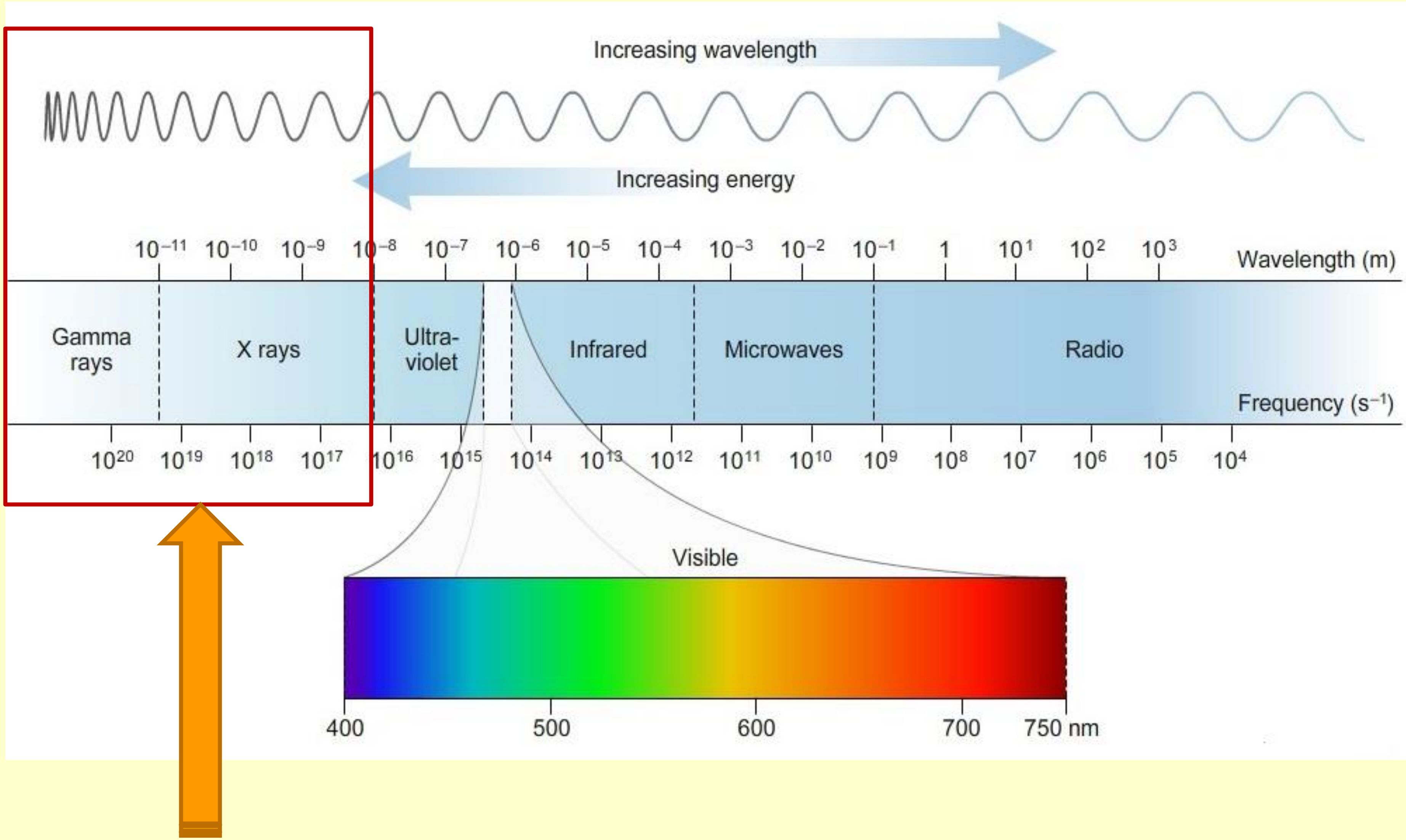

Region of Interest (electromagnetic spectrum) for CT

Introduction to the physical concepts of the tomographic process

- The bases of the X-ray transmission tomography are related to a narrow beam of monoenergetic photons with energy **E** and a flux of photons $\mathbf{N_0}$ passing through a homogeneous body of thickness **x** (in cm):

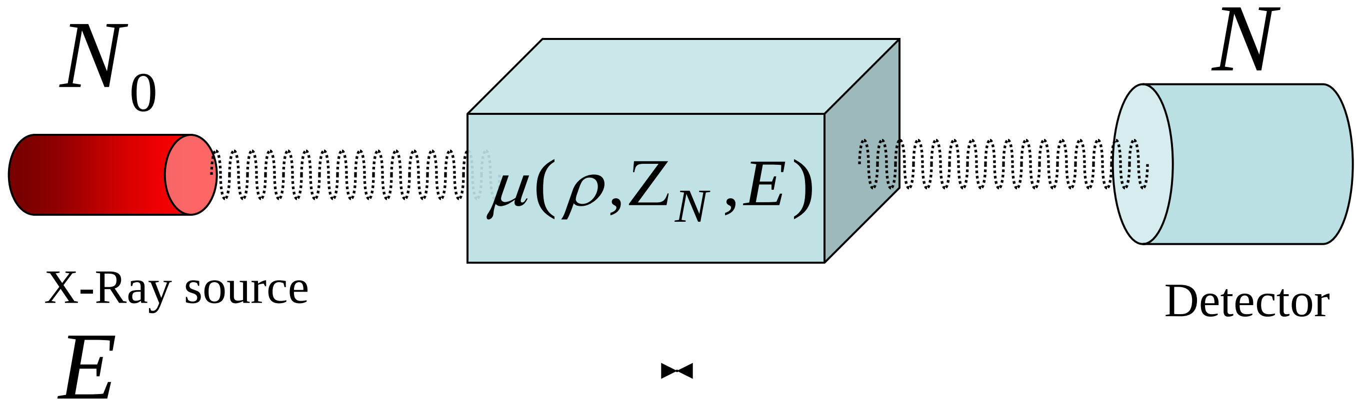

Introduction to the physical concepts of the tomographic process

Attenuated photons intensity

Initial photons intensity

Linear attenuation coefficient (in cm^{-1})

$$N = N_0 e^{\oint_p (-\mu(\rho, Z_N, E)x)dp}$$

Atomic number

Material density (g/cm^3)

• If the study body is a chemical component or a mixture, its mass attenuation coefficient can be roughly evaluated from the coefficients of the elements.

Introduction to the physical concepts of the tomographic process

$$\frac{\mu}{\rho} = \sum_i w_i \left(\frac{\mu_i}{\rho_i} \right)$$

where w_i is proportional to the weight of the i_{th} constituent of the material. The mass attenuation coefficient of a component or mixture can be calculated from the mass attenuation coefficient of the components.

Introduction to the physical concepts of the tomographic process

The differences in linear attenuation coefficients for different materials are energy dependent.

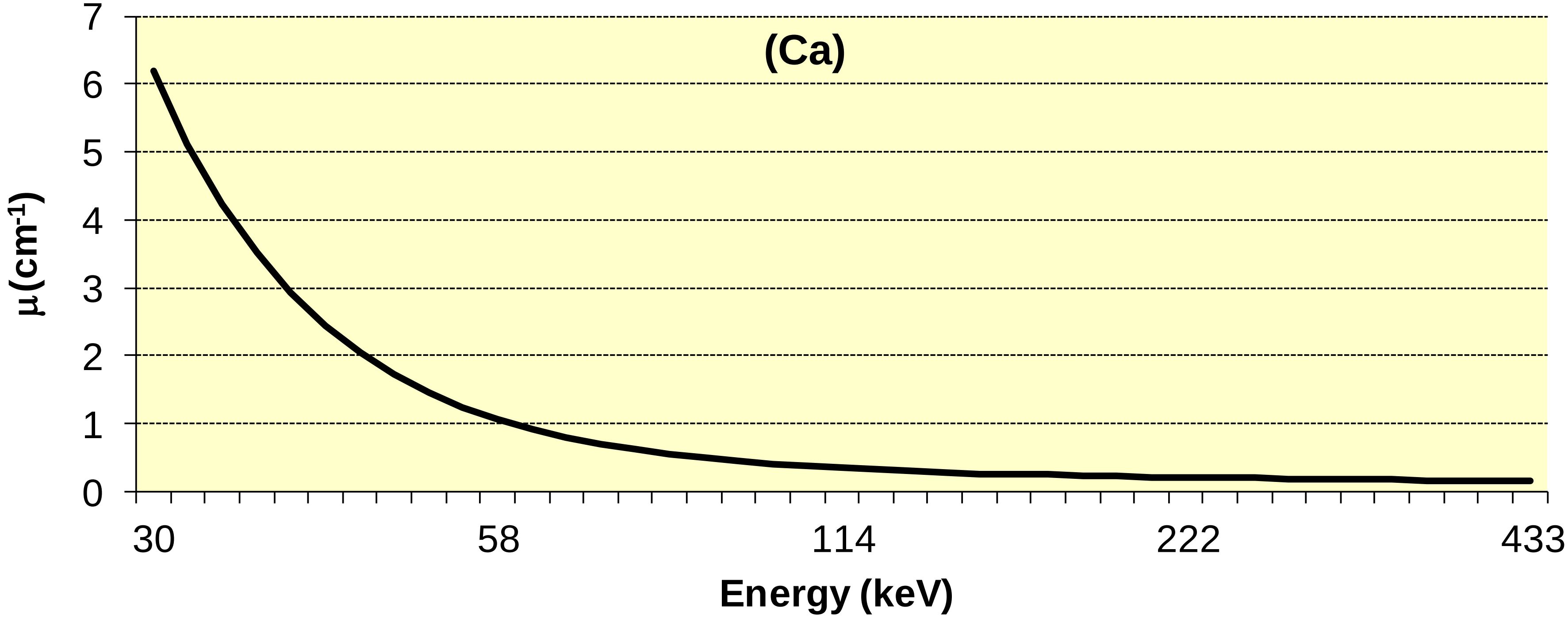

This fact leads to a definition of the contrast in X-ray computed tomography, which is a function of the linear attenuation coefficient values and the mapping process.

Introduction to the physical concepts of the tomographic process

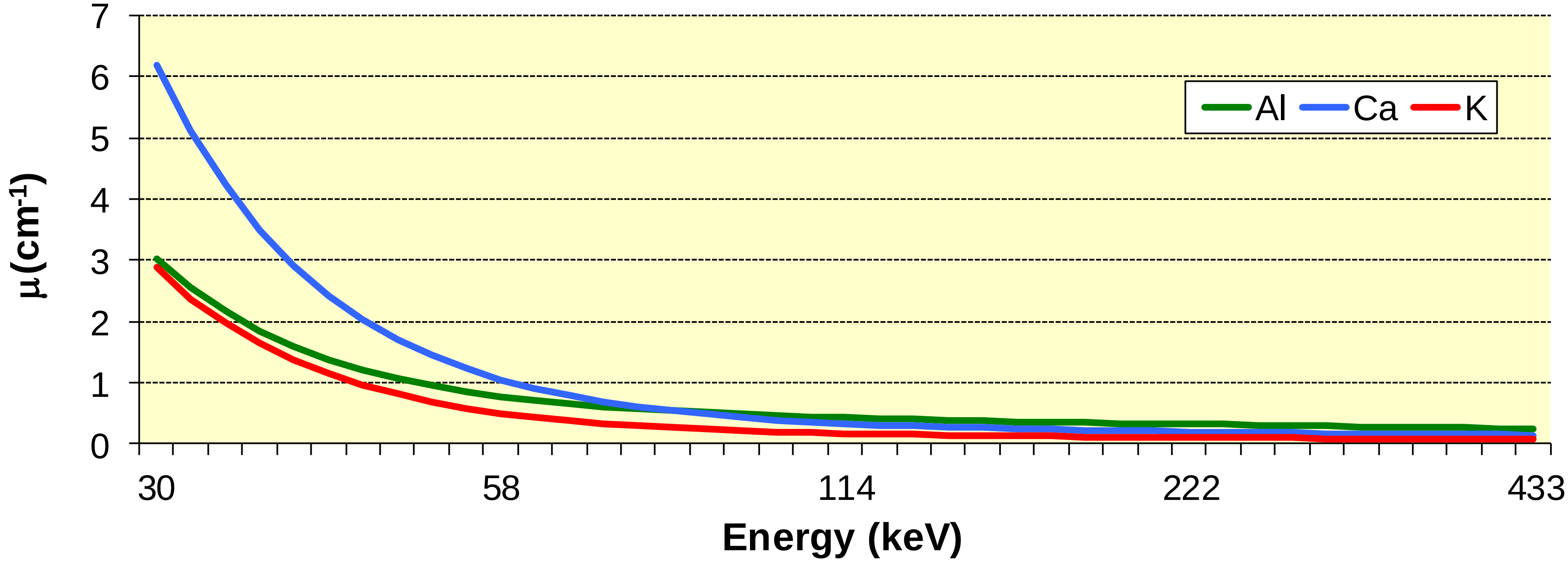

The quality of a tomographic image is correlated to the work energy, as well as the physical characteristics of the samples or bodies under analysis (function of the chemical constituents).

Noise (most significant) of the tomographic process - Poisson noise

- The probability of detecting N photons in an exposure time interval t can be estimated by the Poisson probability distribution function, given by:

Quantum efficiency of the X-Ray detector

Mean ratio of photons (photons/second)

$$\overline{N}_0 = \xi R t$$

The uncertainty or noise is given by the standard deviation, given by:

$$\sigma = \sqrt{\overline{N}_0}$$

An event can occur 0, 1, 2, … times in an interval. The average number of events in an interval is designated λ. It is the event rate, also called the rate parameter. The probability of observing k events in an interval is given by the equation:

$$P(k,t) = \frac{\lambda^k e^{-\lambda}}{k!}$$

Probability mass function (PMF) for a Poisson distribution

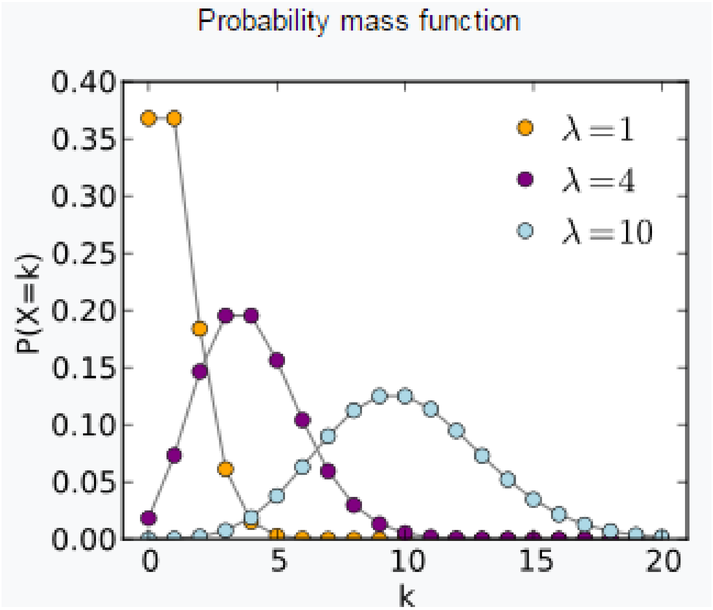

where:

- λ is the average number of events per interval
- *e* is the number 2.71828... (Euler's number) the base of the natural logarithms
- *k* takes values 0, 1, 2, …
- $k! = k \times (k - 1) \times (k - 2) \times \ldots \times 2 \times 1$ is the factorial of *k*.

Sample scanning process

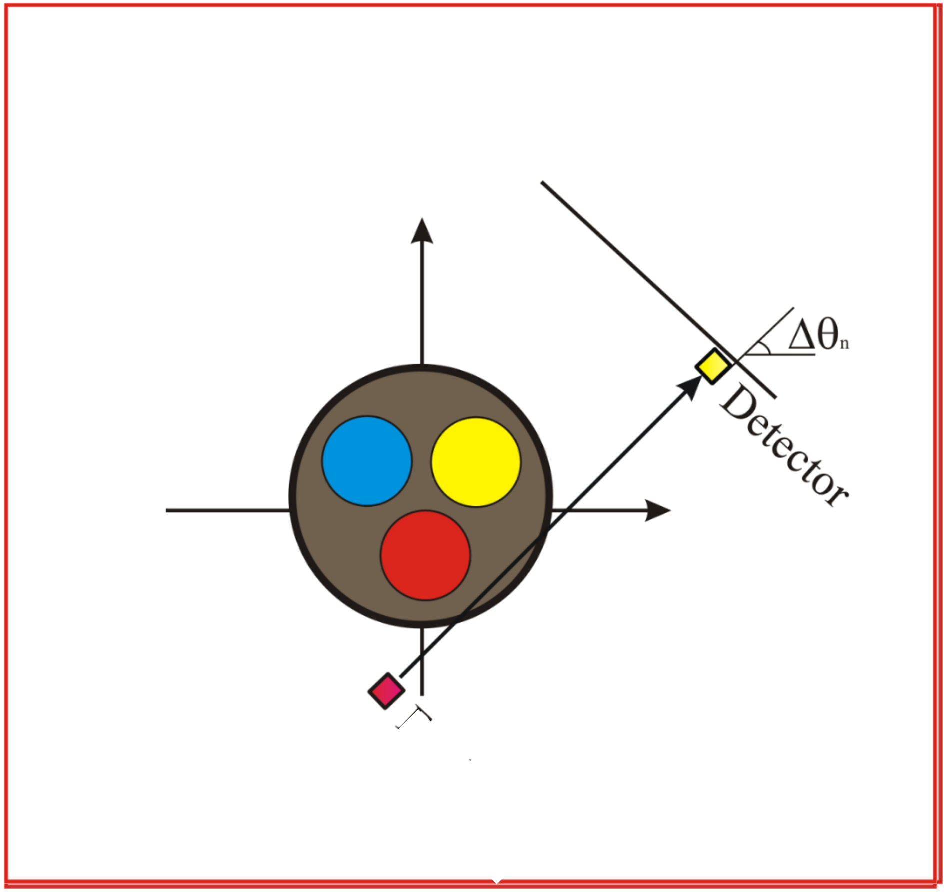

- Two-dimensional reconstruction algorithms use projections to reconstruct the tomographic sections;

- Projections are collected in the interval

$$0^{\circ} \leq \theta < 180^{\circ}$$

i.e., getting the Radon transform of the object;

- Through the inverse transform of Radon one can obtain the reconstructed image of the object, based on the attenuation coefficients

Image Reconstruction from Projections

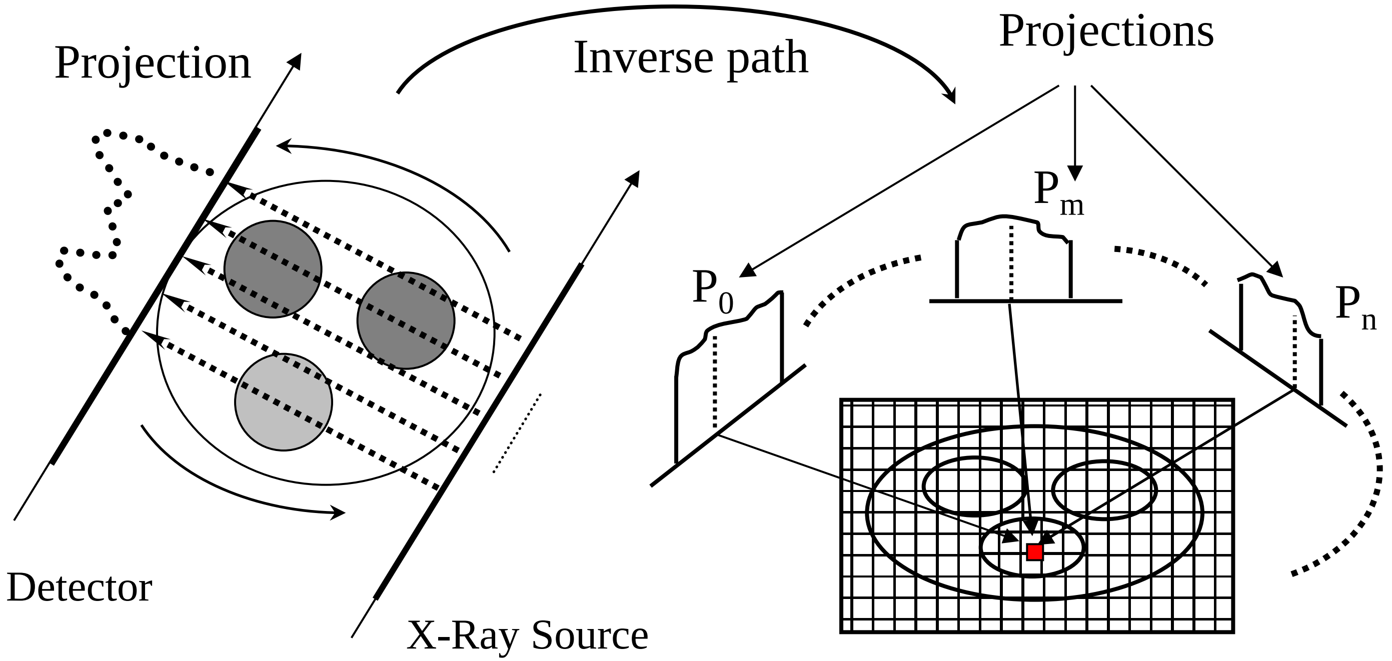

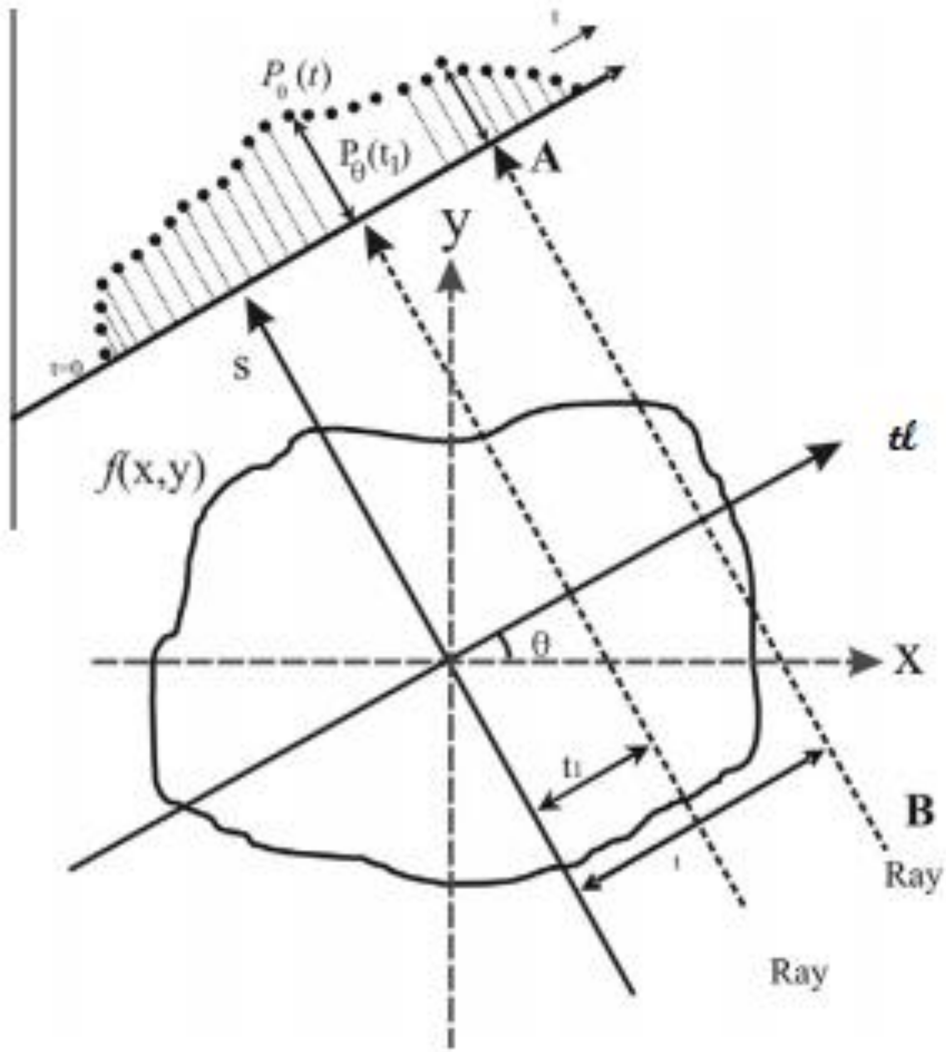

Parallel projection of $f(x, y)$ for Radon Transform.

Considering the time domain and take into account the Inverse Fourier Transformation

$$f(x,y)=\int_{-\infty}^{\infty}\int_{-\infty}^{\infty}F(u,v)e^{j2\pi(ux+uy)}dudv$$

Changing from rectangular coordinate system (u, v) to polar coordinate system (ω,θ) and changing the differential variables

$$dudv=\omega d\omega d\theta$$

$$f(x,y)=\int_{0}^{2\pi}\int_{0}^{\infty}F(\omega,\theta)e^{j2\pi\omega(x\cos\theta+y\mathrm{sen}\theta)}\omega d\omega d\theta$$

Using discrete forms to represent de projections and rewritten the equations in the frequency domain, is possible to find:

$$Q_\theta(n\tau) = \tau \times IFFT\left\{FFT[P_\theta(n\tau)] \times FFT[h(n\tau)]\right\}$$

where **τ** is the sampling interval

$$Q_\theta(n\tau) = \tau \times IFFT\left\{FFT[\hat{P}_\theta(n\tau)] \times FFT[h(n\tau)]\right\}$$

$$\hat{f}(x, y) = \frac{\pi}{K} \sum_{i=1}^{K} Q_\theta(x \cos\theta_i + y\, sen\theta_i)$$

Reconstruction from projections

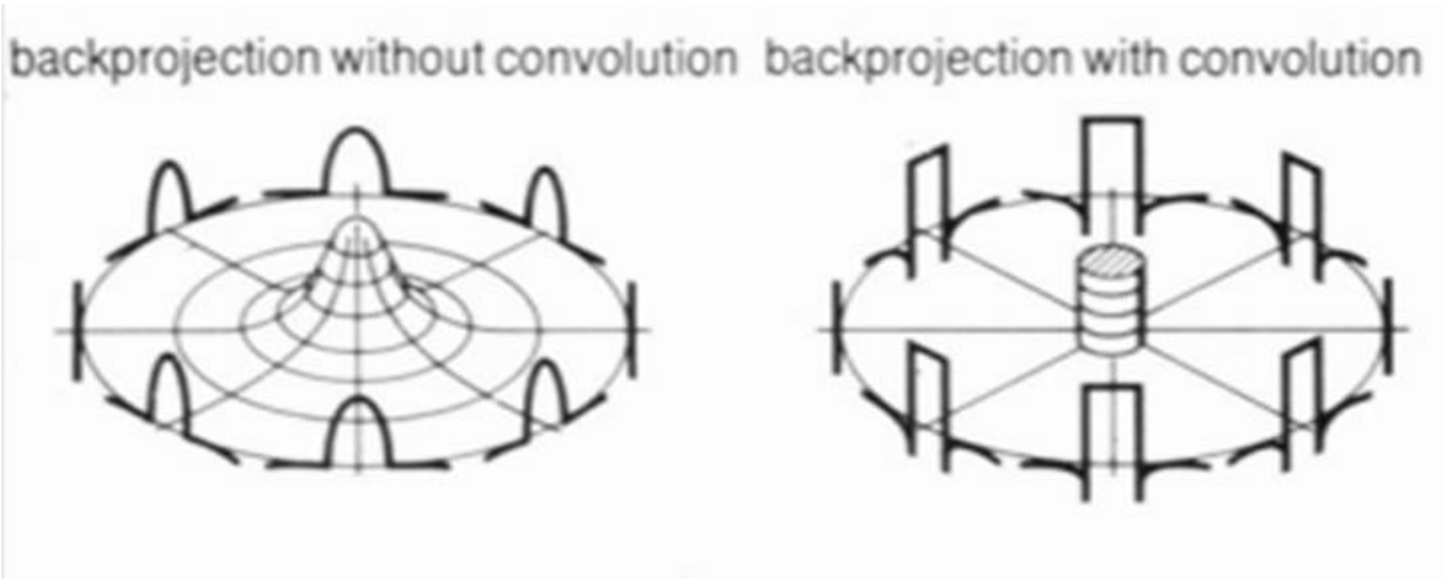

CT without covers

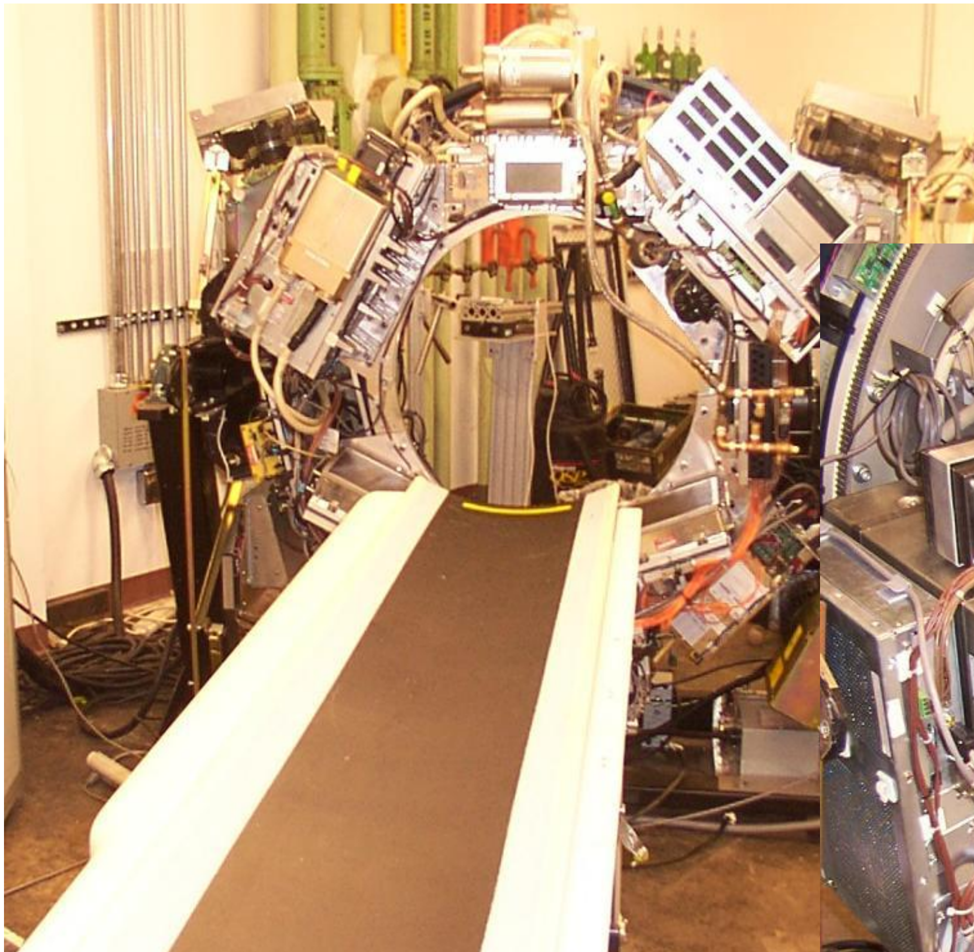

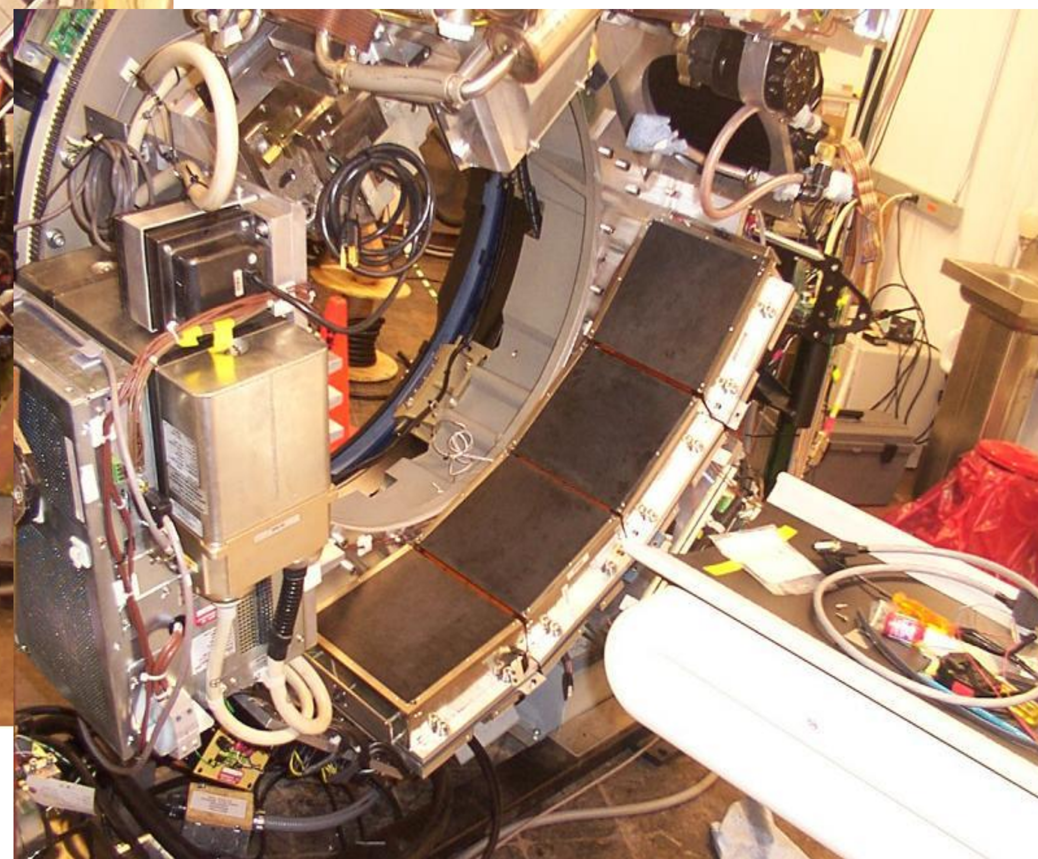

Typical CT architectures

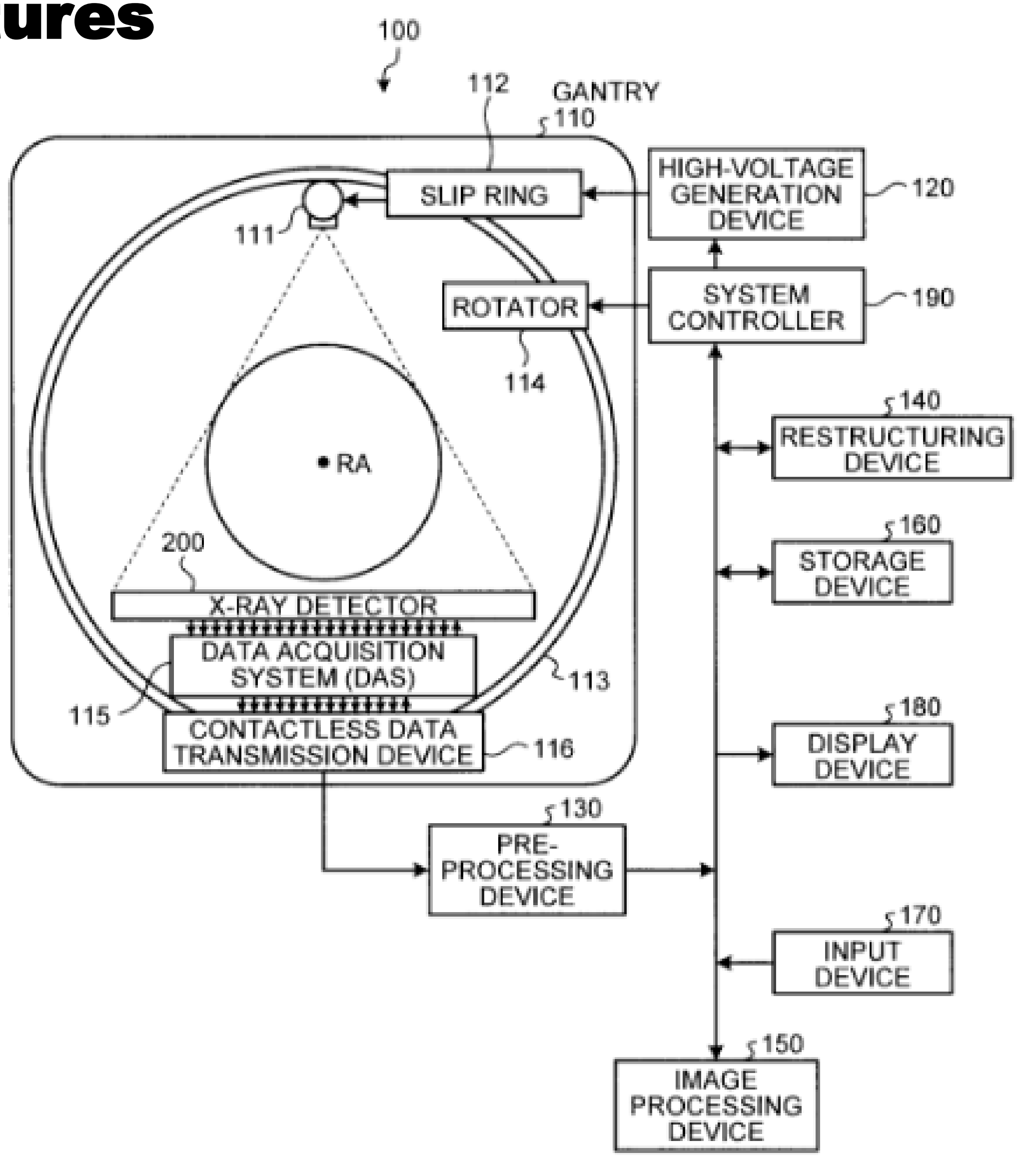

Source: X-ray computed tomography apparatus, radiation detector, and method of manufacturing radiation detector (Patent US 20120069954 A1)

Typical Schematic Representation for Scanning Geometry of a CT System

What are inside the gantry?

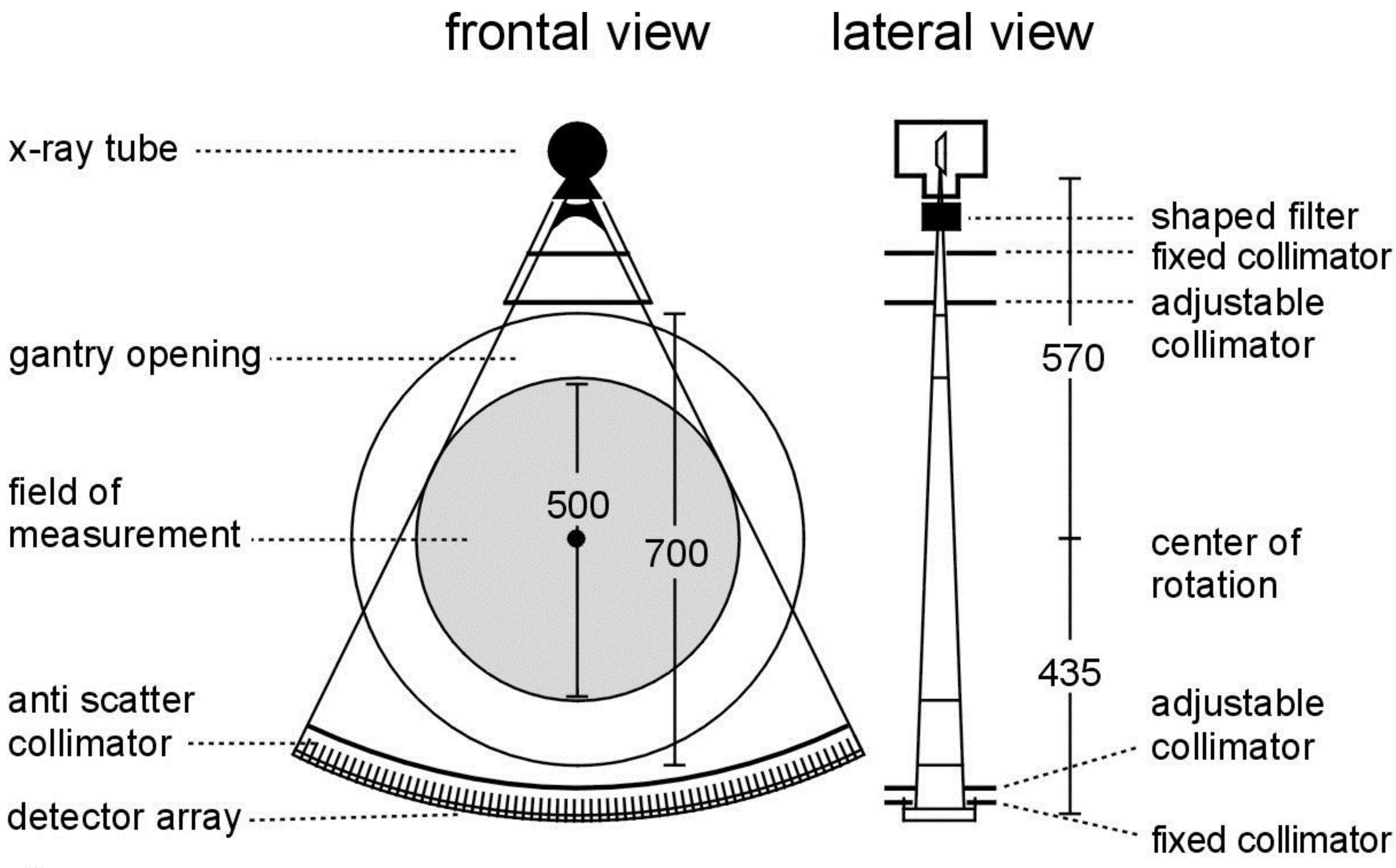

CT System & Generations

Generation	Source	Source Collimation	Detector	Detector Collimation	Source-Detector movement	Advantages
1^{st}	single	Pencil beam	single	no	Translation + Rotation	No scatter
2^{nd}	single	Fan-beamlet	multiple	yes	Translation + Rotation	Faster than 1^{st} Generation
3^{rd}	Single	Fan-beam	many	no	Rotates together	Faster than 2^{nd} Generation
4^{th}	Single	Fan-beam	Stationary ring	no	X-Ray Source rotates only	Higher efficiency than 3^{rd} Generation
5^{th}	multiple	Fan-beam	Stationary ring	no	No movement	Ultrafast for dynamic analysis (for instance in cardiac movements
6^{th}	single	Fan-beam	many	yes	3^{rd} Generation +bed translation	Faster 3D imaging
7^{th}	single	Narrow cone-beam	Multiple arrays	yes	3^{rd} Generation +bed translation	Faster 3D imaging
8^{th}	single	Wide cone-beam	Flat Panel detector (FDP)	no	3^{rd} Generation	Large 3D

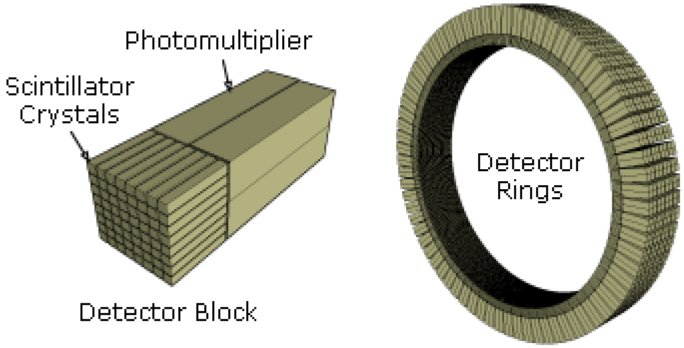

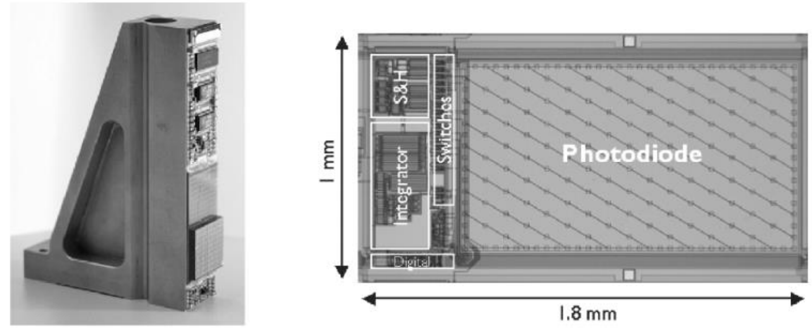

CT Detector module based on integrated CMOS photodiodes

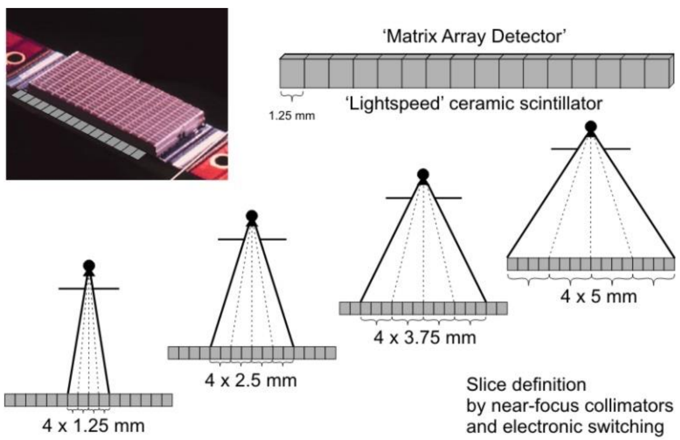

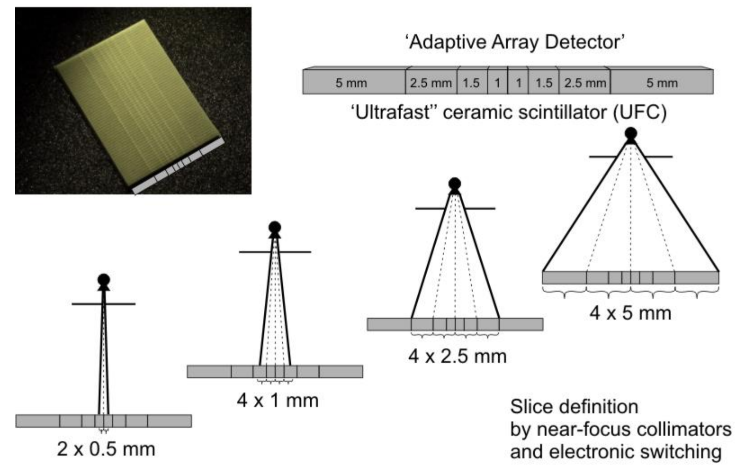

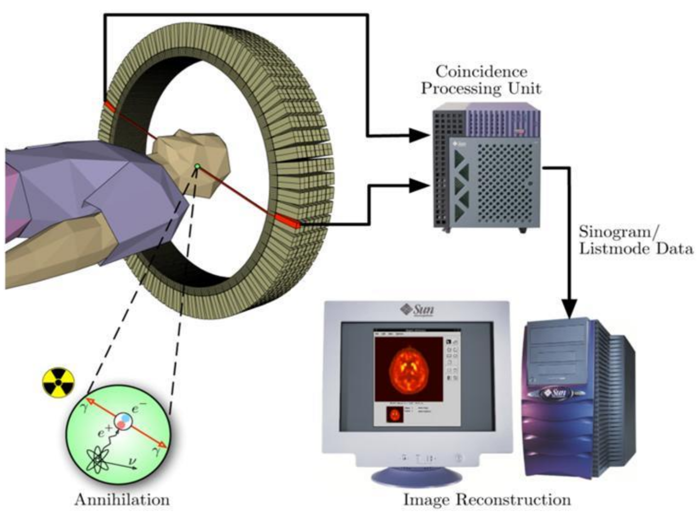

(Helical CT)

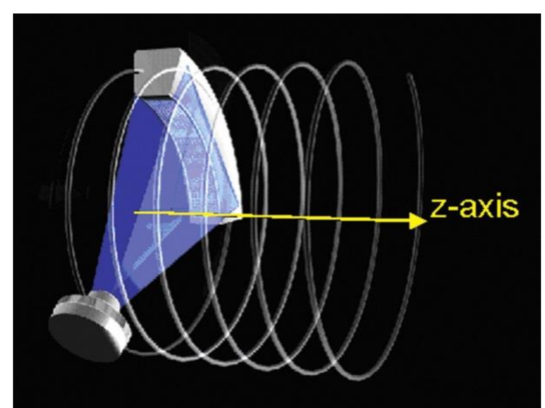

SNR vs. Dose

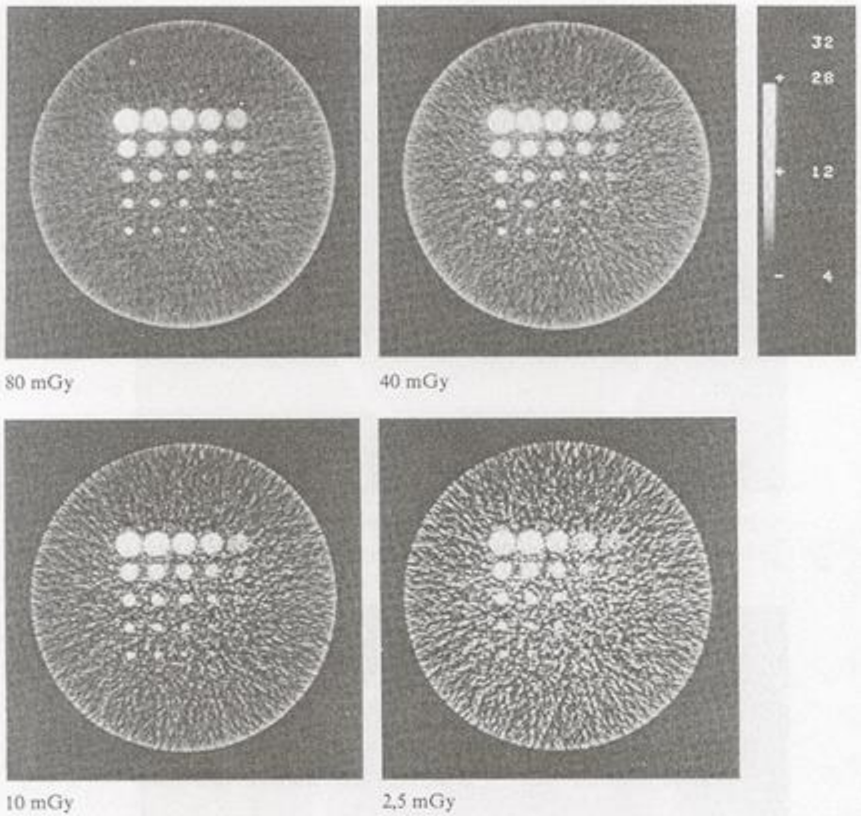

Fig. 4.24
"Button card": rods in the water bath. The density of the rods decreases from left to right. The preferential radial direction of the noise islands at the edge of the object should be noted. The dose per slice image is given in milliGrays (mGy)

SNR is dependent on dose, as in X-ray. Notice how images become grainier and our ability to see small objects decreases as dose decreases.

Source: Imaging Systems for Medical Diagnosis: Fundamentals and Technical Solutions - X-Ray Diagnostics- Computed Tomography - Nuclear Medical Diagnostics - Magnetic Resonance Imaging - Ultrasound Technology, by Erich Krestel (Editor), pp. 627. ISBN 3-8009-1564-2. Wiley-VCH , October 1990.

CT in Agriculture

- In 1982 and 1983 studies were conducted respectively by Petrovic & Hainsworth, and Aylmore. They demonstrated the possibility of using a computerized X-ray tomograph to measure the bulk density of soils;

- In 1986, Crestana and collaborators presented results related to the applications of CT in agriculture for:

1. Detection of soil heterogeneities;
2. Compaction of soils resulting from the use of agricultural machinery;
3. Dynamic three-dimensional simulation of drip irrigation in a soil column;
4. Studies on seed germination in situ.

Their results were compared with usual techniques in the agricultural area the use of CT showed greater precision.

Crestana, S.; Mascarenhas, S.; Pozzi-mucelli, R.S. Static and dynamic three-dimensional studies of water in soil using computed tomographic scanning. Soil Science, v.140, p.326-332,1985.; Aylmore, L. A. G. Use of computer-assisted tomography in studying water movement around plant roots. Advances in Agronomy, San Diego, v. 49, p. 1-53, 1993.; Petrovic, A.M.; Siebert, J.E.; Rieke, P.E. Soil bulk density analysis in three dimensions by computed tomographic scanning. Soil Science Society of America Journal, v.46, p.445-450, 1982.

CT in Agriculture

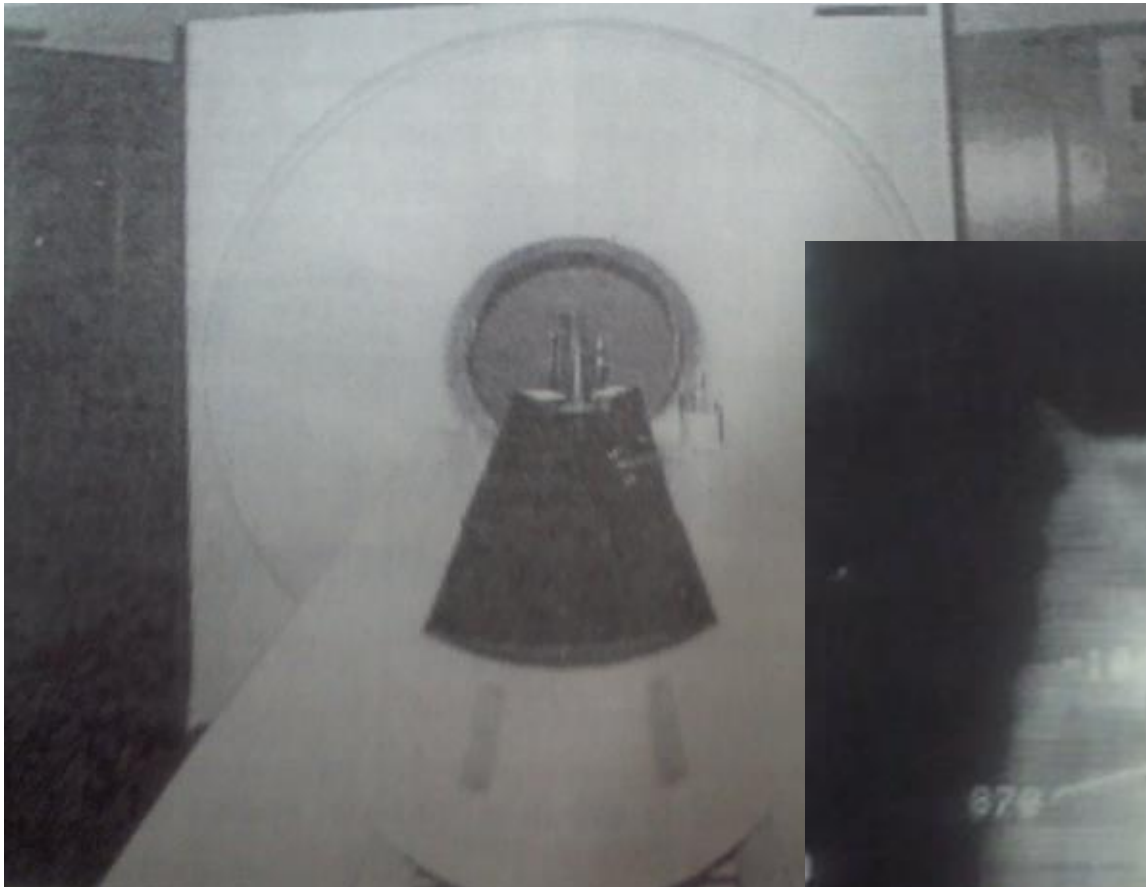

CT in Agriculture

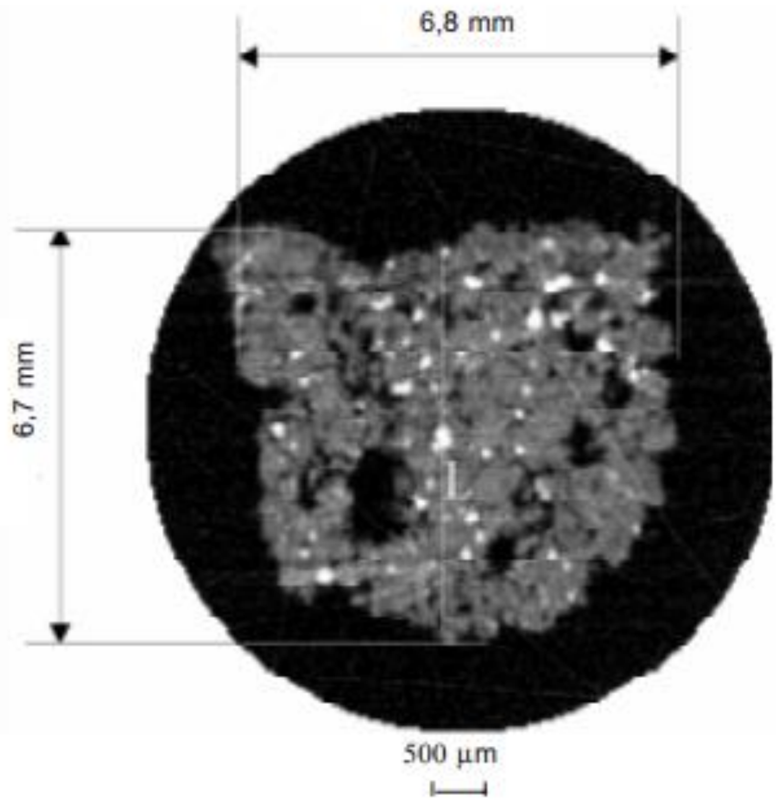

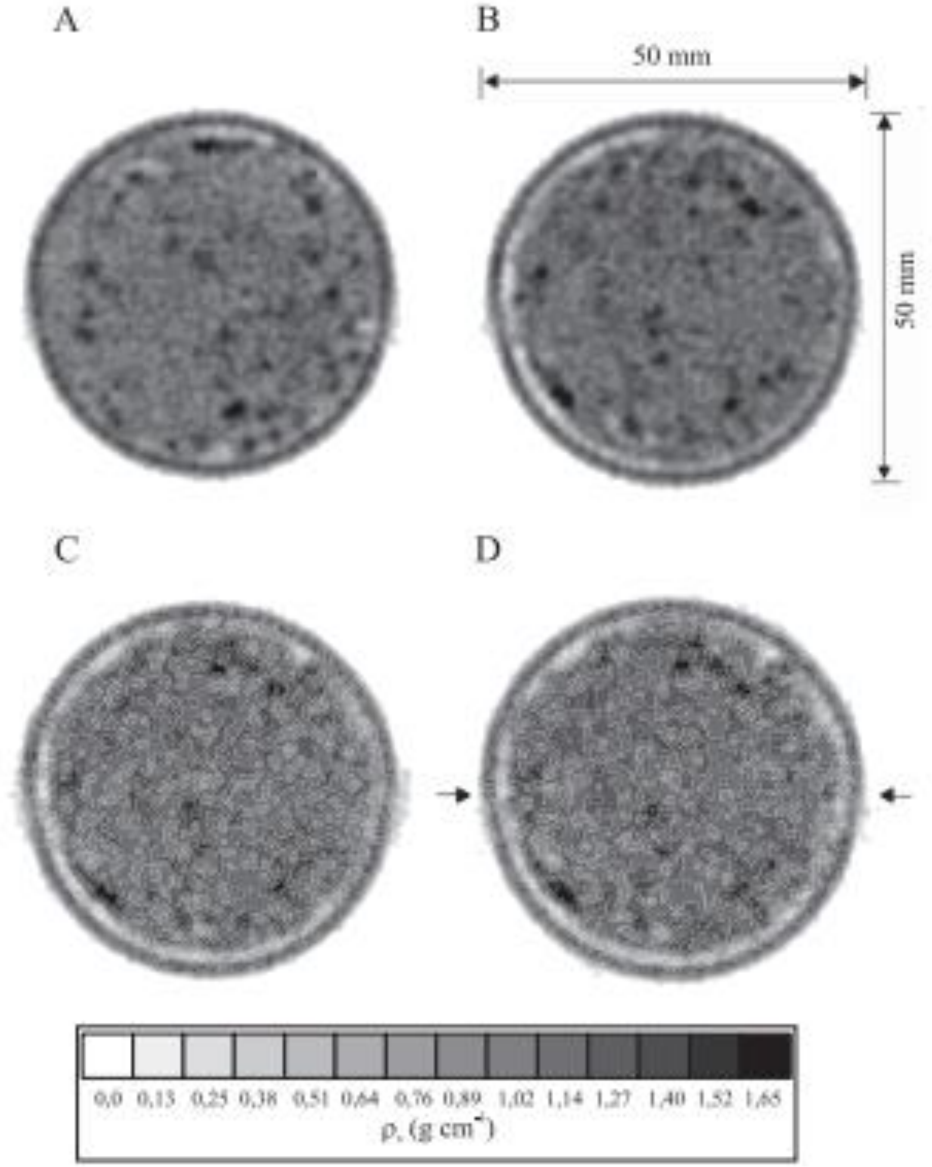

CT in Agriculture

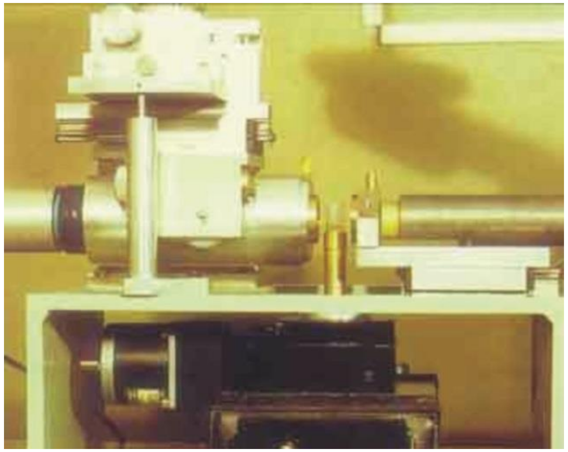

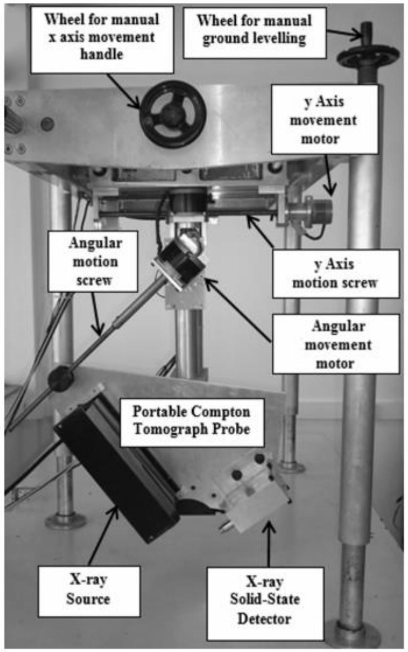

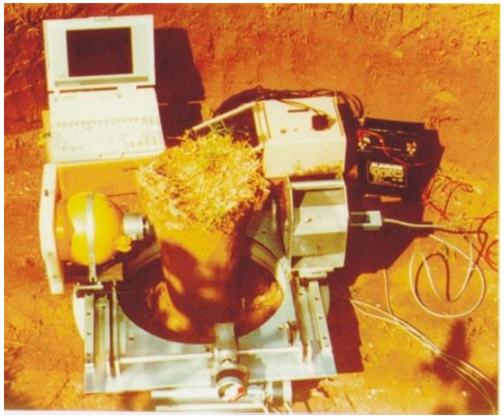

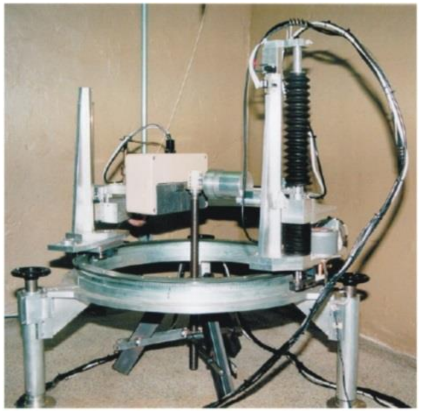

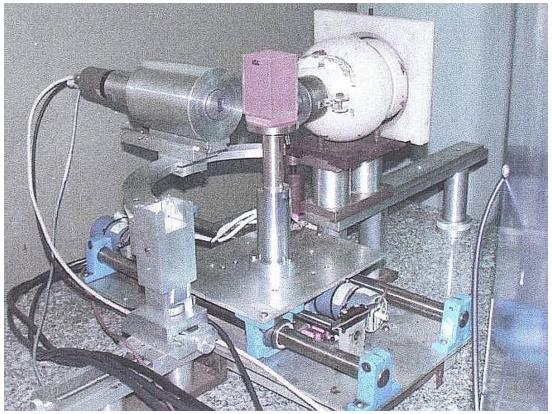

Cruvinel, P.E., Cesareo, R., Crestana, S., Sergio Mascarenhas (1990) X-and Gamma-rays computerized minitomograph scanner for soil science. IEEE Trans. Instrum. Meas. 39 (5), 745–750;
Naime, J.M., Cruvinel, P.E., Crestana, S., Conciani, M.M., Soares, W., Gazzinelli, R., Moreira, R.L., Rodrigues, W.N., (1997). Portable cat scanner applied to collapsible soil studies. In: 2nd International Conference on Physics and Industrial Development: Bridging the Gap. pp. 327–331C;
Macedo, A., Cruvinel, P.E., Inamasu, R.Y., Jorge, L.A.C., Naime, J.M., Torre-Neto, A., Vaz, C.M.P., Crestana, S., (1999). Micrometric X-ray ct scanner dedicated to soil investigation. In: IEEE International Multiconference on Circuits, Systems, Communications and Computers. vol. 3.;
Balogun, F., Cruvinel, P., (2003). Compton scattering tomography in soil compaction study. Nucl. Instrum. Methods Phys. Res., Sect. A 505 (1), 502–507.

Model and Algorithm Conception

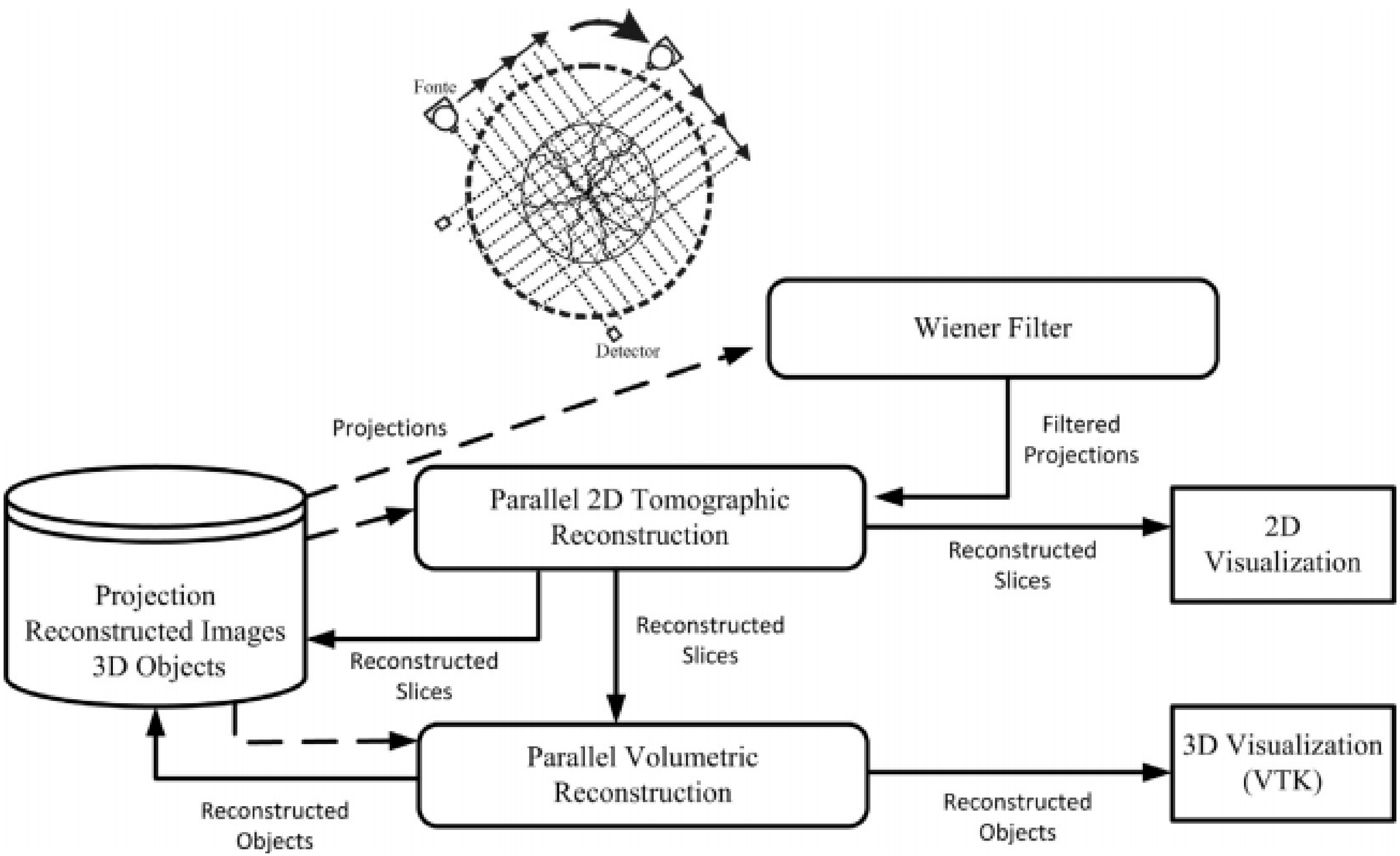

Diagram with the high level model of work processes.

Filtering Prior to Image Reconstruction

- One of the main problems in CT measurement is the improvement of the Signal/Noise ratio of the collected projections and the reconstructed image. This involves:

1. Poisson noise;
2. Noise from electronics;
3. Table vibrations;
4. Noise of reconstruction and visualization algorithms.

Filtering Prior to Image Reconstruction

- Regarding Poisson noise, the possible solutions are:

1. Increase the exposure time to radiation, to improve the signal-to-noise ratio;
2. Applying filtering to reduce Poisson noise, working on the projections, or a posteriori in the reconstructed image.

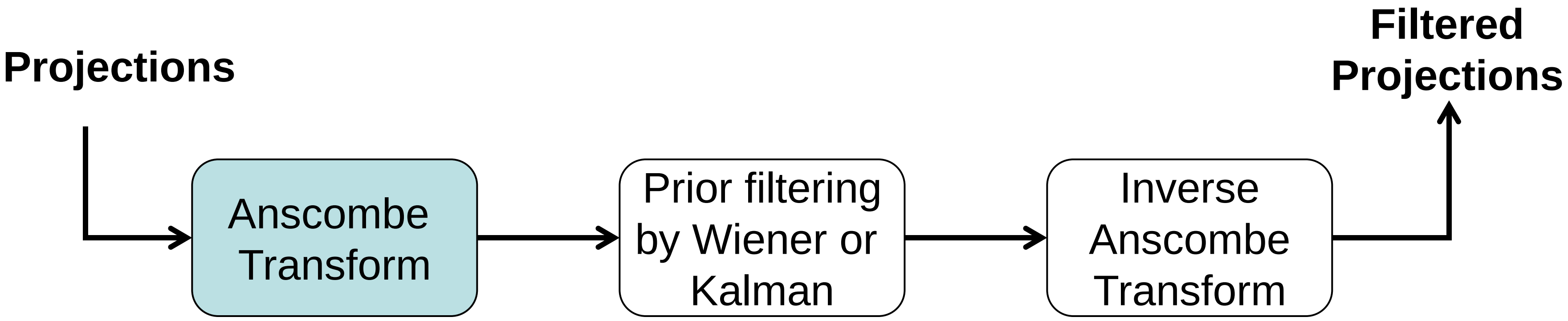

Why to use Anscombe Transform?

- Poisson noise is characterized by being signal dependent;

- By means of the Anscombe (AT) Transform the Poisson noise is transformed into one that is approximately Gaussian, additive, with zero mean and unit variance [Anscombe, 1948] [Mascarenhas et al, 1999];

- Enables the use of noise reduction methods with stationary Gaussian distribution.

- For the random variable x (Poisson distribution) its AT will be defined as:

$$y_i = 2\sqrt{x_i + \frac{3}{8}} \Leftrightarrow y_i = 2\sqrt{x_i + \frac{1}{8}} + v_i$$

$$s_i$$

Approximately independent

Filtering Prior to Image Reconstruction (using Wiener)

- In the 1940s, Norbert Wiener pioneered a filter that would produce an optimal estimate of a noisy signal [Wiener, 1949]:

$$x(n) = d(n) + v(n)$$

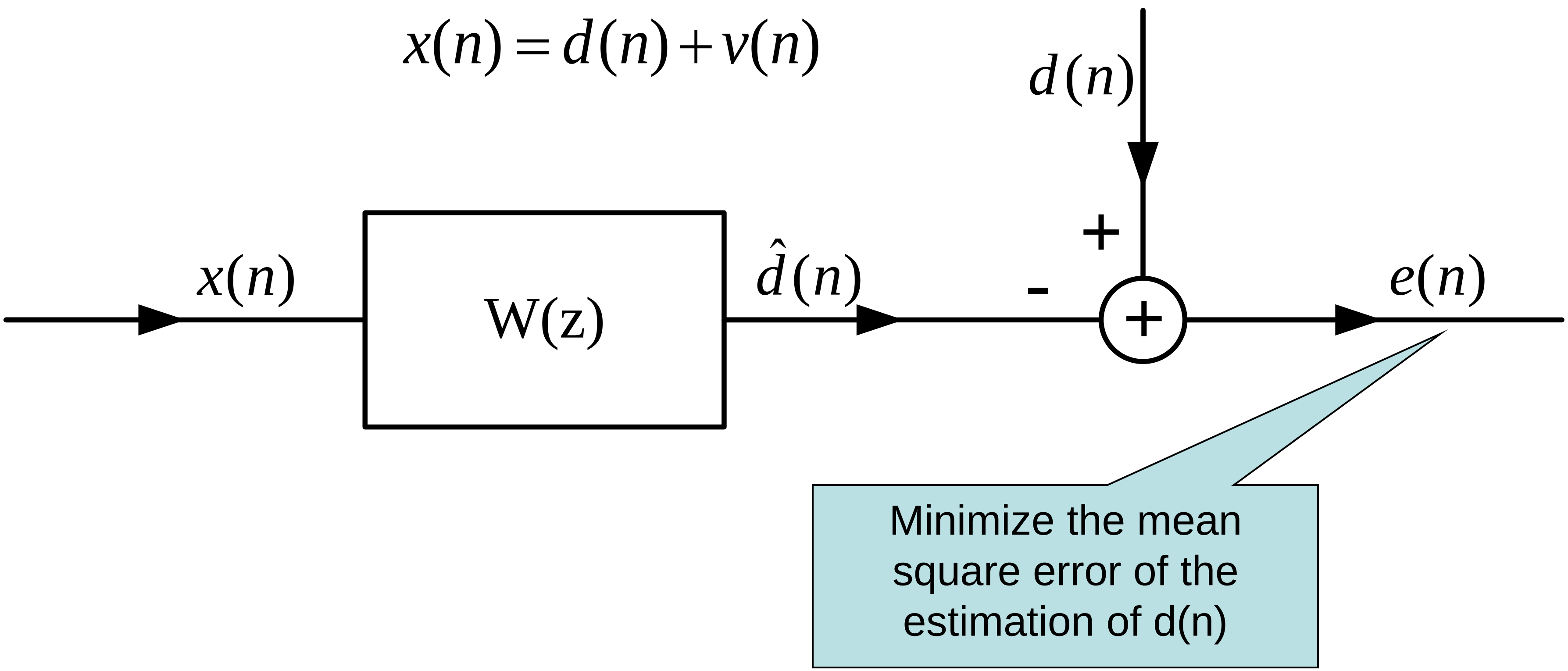

Filtering Prior to Image Reconstruction (using Wiener-FIR)

- For a FIR filtering, one may have the systems of Wiener-Hopf equations given by:

$$\begin{bmatrix} r_x(0) & r_x(1) & \cdots & r_x(p-1) \\ r_x(1) & r_x(0) & \cdots & r_x(p-2) \\ \cdots & \cdots & \cdots & \cdots \\ r_x(p-1) & r_x(p-2) & \cdots & r_x(0) \end{bmatrix} \begin{bmatrix} w(0) \\ w(1) \\ \cdots \\ w(p-1) \end{bmatrix} = \begin{bmatrix} r_{dx}(0) \\ r_{dx}(1) \\ \cdots \\ r_{dx}(p-1) \end{bmatrix}$$

Autocorrelation of the signal

Weights for the FIR filter

Cross-correlation between the desired signal d(n) and the input x(n)

Wiener Filtering by Linear Prediction

- From observations without noise it is sought to estimate the value of $\hat{x}(n+1)$ in terms of a linear combination of p values prior to $x(n+1)$

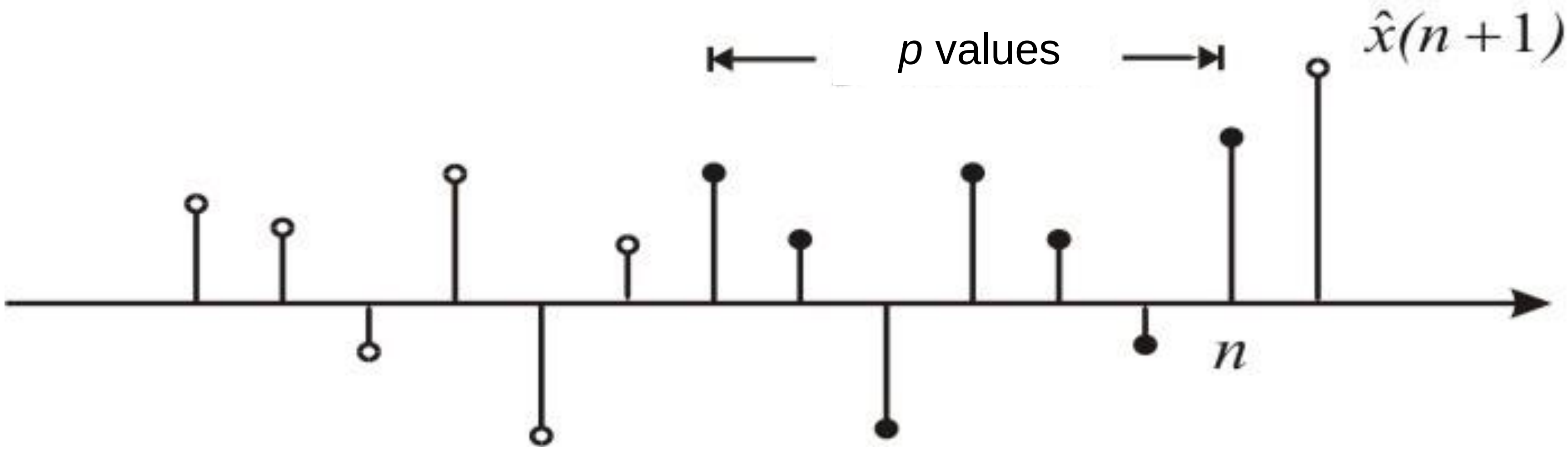

Re-evaluating the cross-correlation between d(n) and x(n), is possible to obtain:

$$r_{dx}(k) = r_x(k+1)$$

Thus, the Wiener-Hoft equations for the linear predictor are defined as:

$$\begin{bmatrix} r_x(0) & r_x(1) & \cdots & r_x(p-1) \\ r_x(1) & r_x(0) & \cdots & r_x(p-2) \\ \cdots & \cdots & \cdots & \cdots \\ r_x(p-1) & r_x(p-2) & \cdots & r_x(0) \end{bmatrix} \begin{bmatrix} w(0) \\ w(1) \\ \cdots \\ w(p-1) \end{bmatrix} = \begin{bmatrix} r_x(1) \\ r_x(2) \\ \cdots \\ r_x(p) \end{bmatrix}$$

3D Reconstruction for Agricultural Soil Samples

- Tomographic data are acquired without displacement of the sample under analysis. The position during the scanning process remains the same;

- Completion of the intervals between acquisition plans (A) and virtual plans (V);

- This feature allows to use interpolation and to increase resolution of 3D objects, i.e., called as Volumetric Reconstruction

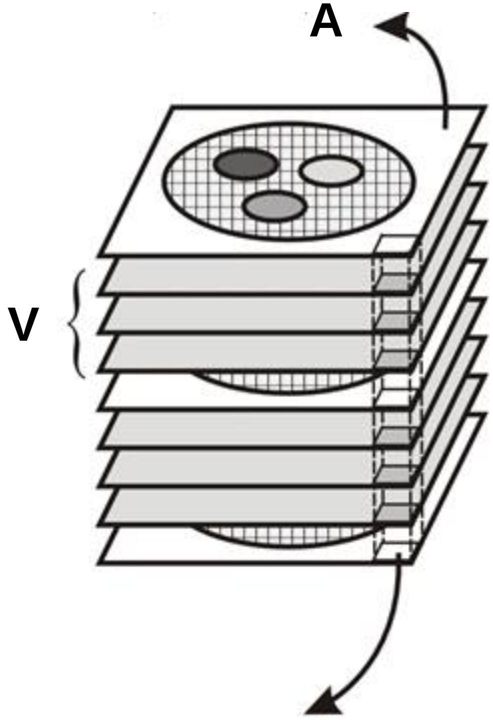

Aligned pixels used
In the process of interpolation

3D Reconstruction of Agricultural Samples - B-Spline-Wavelet Interpolation

- Function for interpolation

$$f(u) = \sum_{i=0}^{N} a_i B(Nu - i)$$

Where u represents the step in interpolation and N is the number of known points

Blending Function

$$B(x) = \begin{cases} \frac{1}{6}(2+x)^3 & -2 < x \le -1 \\ \frac{1}{6}\left(4 - 6x^2 - 2x^3\right) & -1 < x \le 0 \\ \frac{1}{6}\left(4 - 6x^2 + 2x^3\right) & 0 < x \le 1 \\ \frac{1}{6}(2-x)^3 & 1 < x < 2 \\ 0 & 2 \le |x| \end{cases}$$

3D CT Image Reconstruction (interpolation procedures)

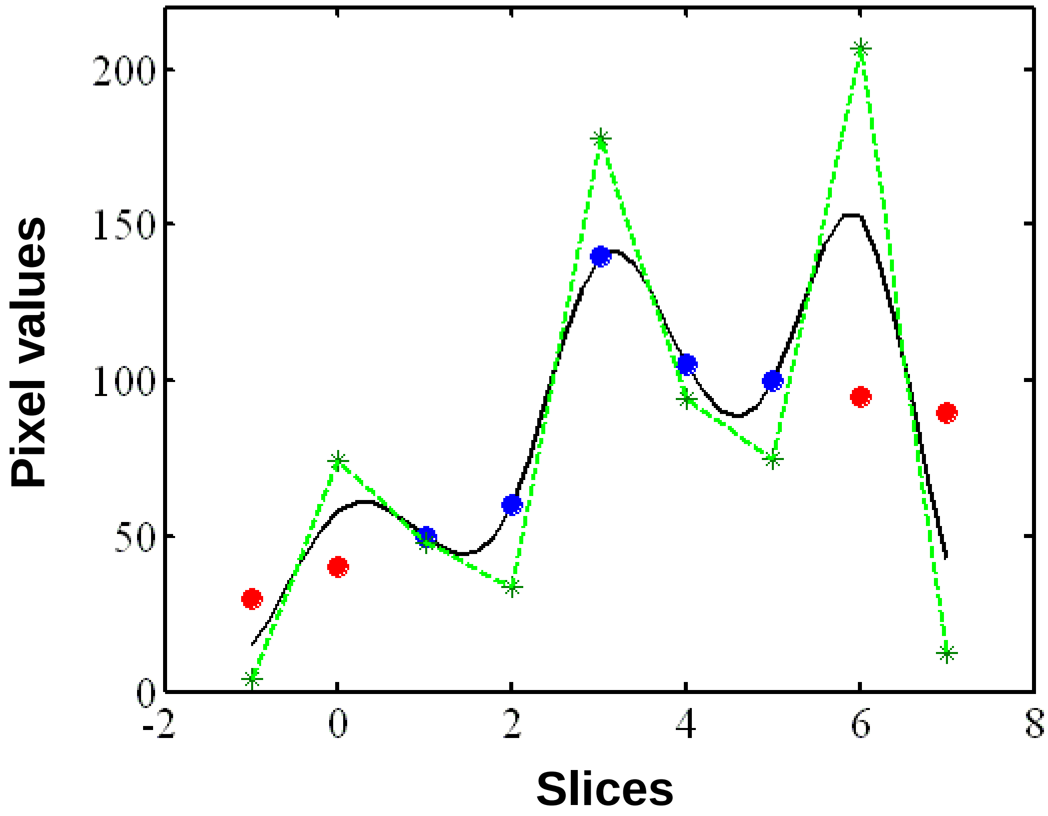

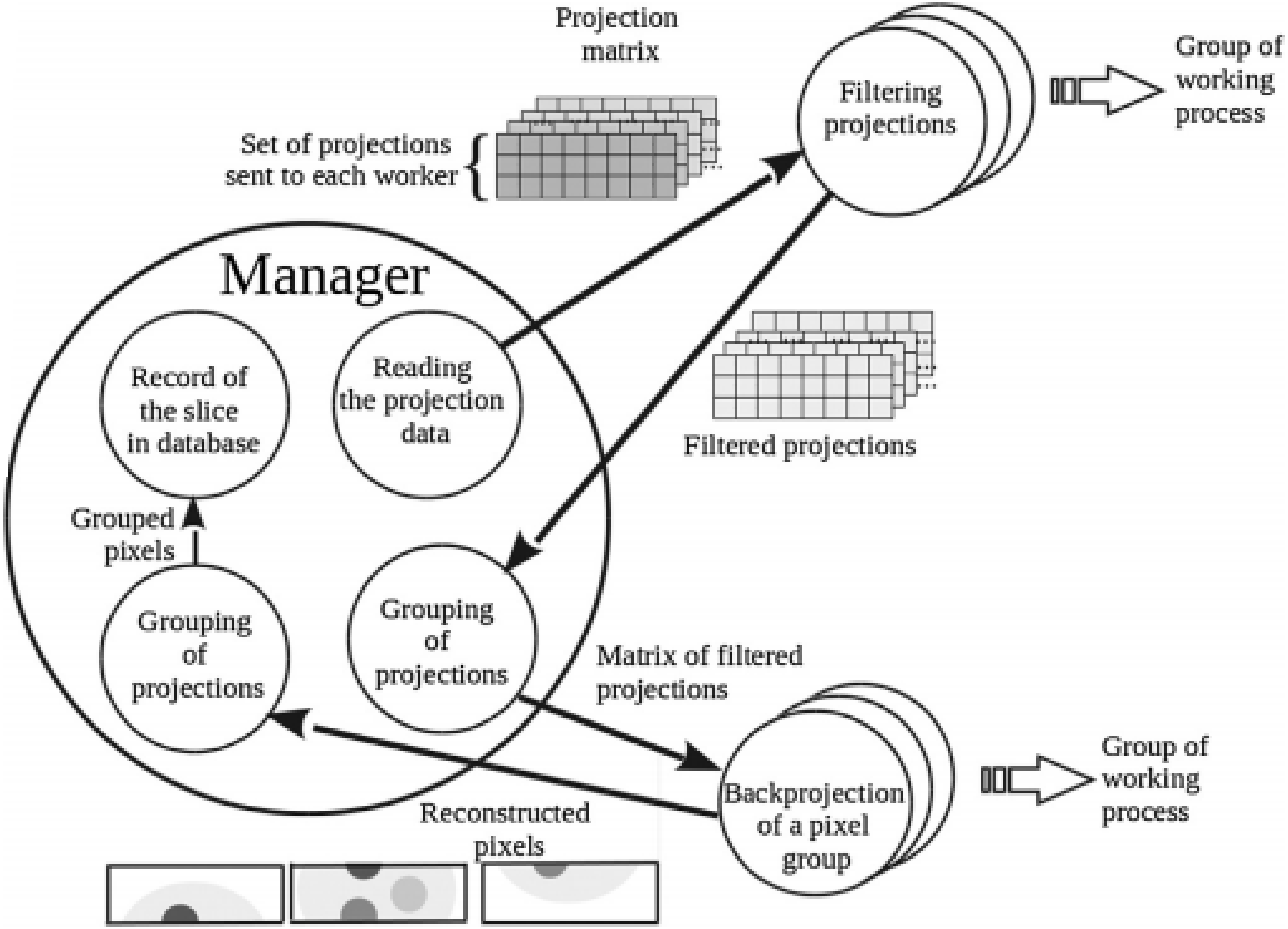

Parallel 2D reconstruction algorithm used in the proposed model.

Source: P.E. Cruvinel ; Pereira, M. F. L. ; Saito, J H ; Costa, L F . Performance Improvement of Tomographic Image Reconstruction Based on DSP Processors. IEEE Transactions on Instrumentation and Measurement, v. 58, p. 3295-3304, 2009.

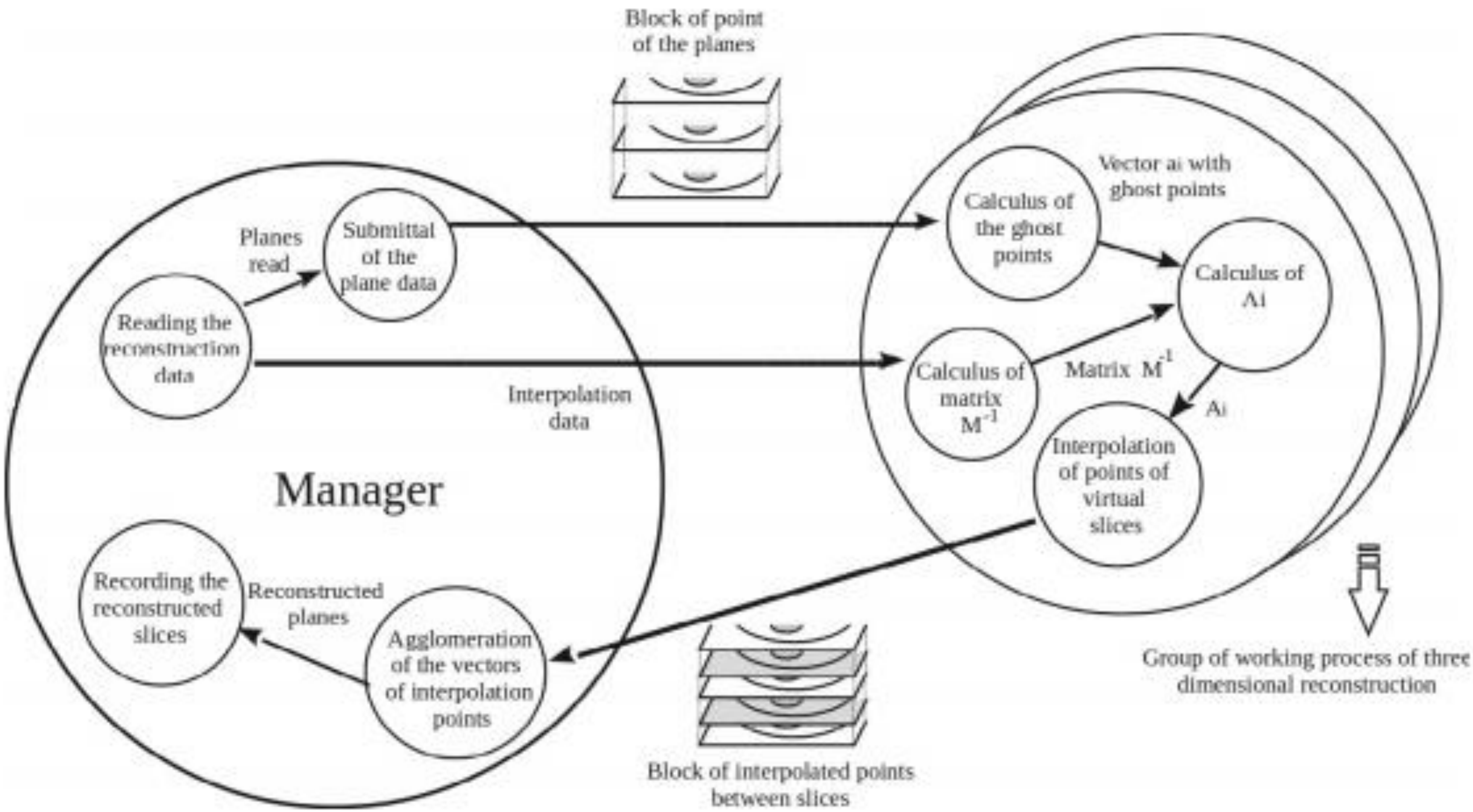

Agglomeration of the parallel three-dimensional reconstruction tasks.

Modeling the parallel algorithm for 2D and 3D reconstruction - Mapping in DSP platform

– Interface between PC and DSP modules

– Interconnection of a network of modules

Source: Hunt Engineering

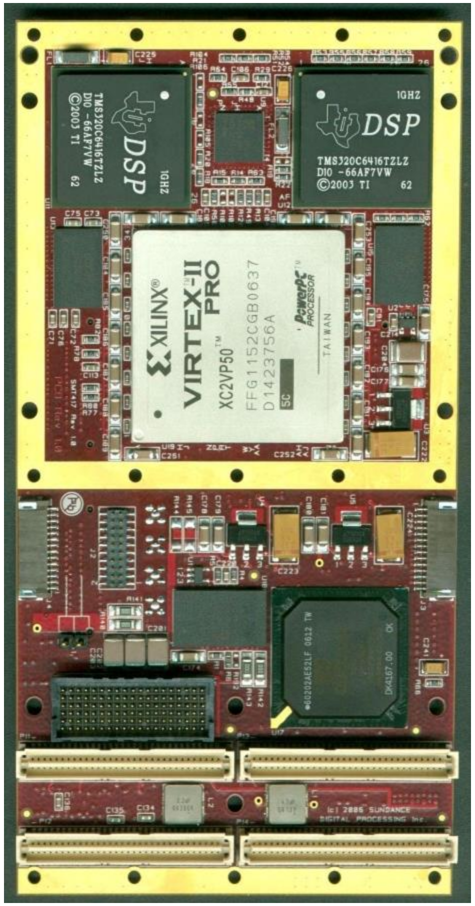

Source: Xilinx Virtex

Filtering with Wiener

- Assays performed with additive Gaussian noise and evaluation based on the resulting variance before and after the filtration;
- In the study, a homogeneous phantom and a heterogeneous phantom were used;

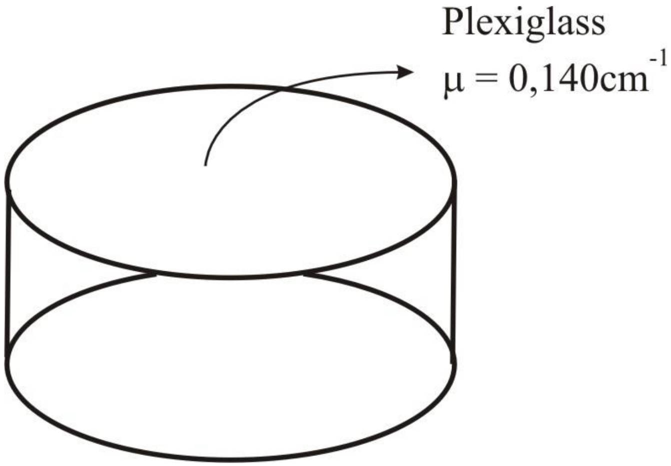

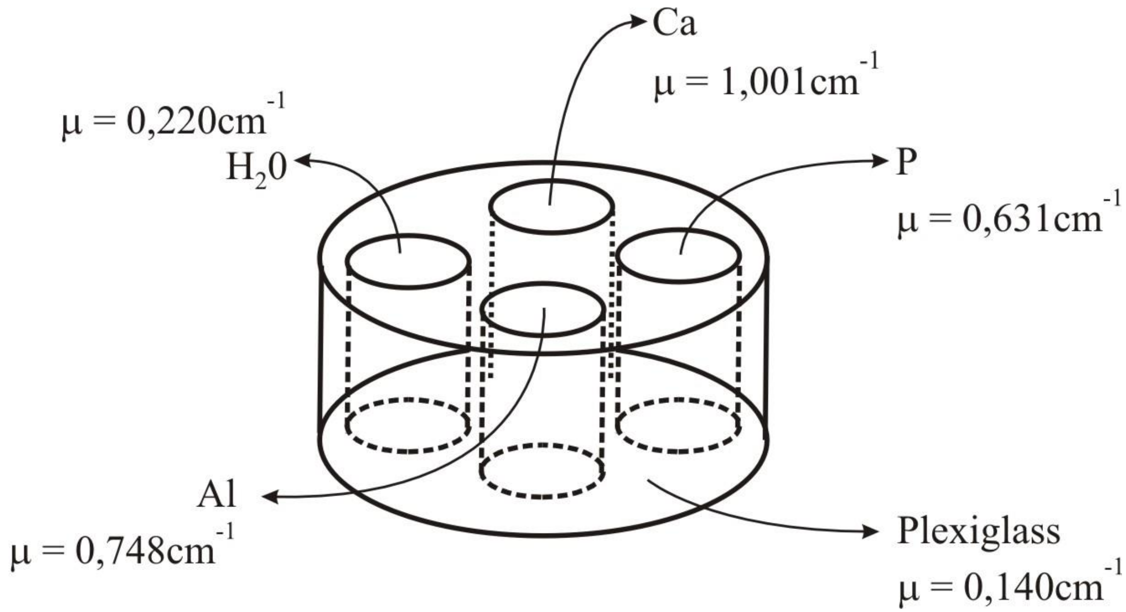

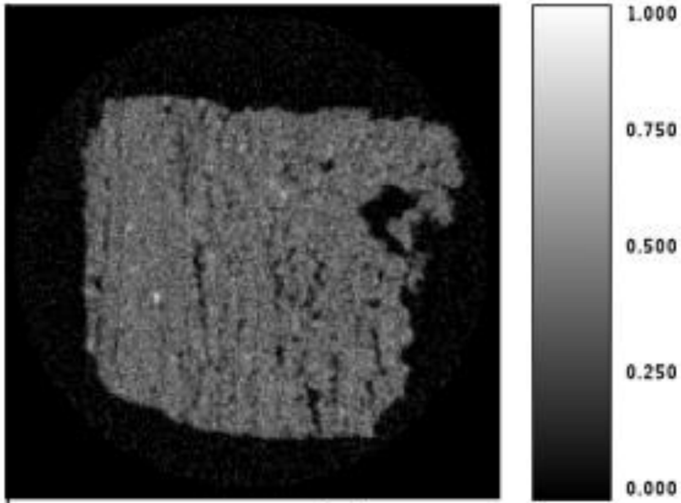

(a)

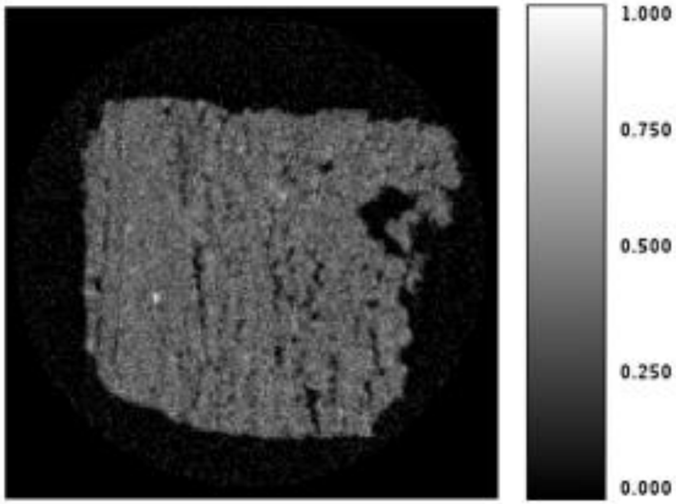

(b)

Fig. 11. Typical reconstructed CT images for the analyzed soil samples, which are the dystrophic clay Dark-Red Latosoil. (a) Noisy image; (b) Filtered image with the Wiener filter based on the linear prediction with 6 weights.

Source: M.F.L. Pereira, P.E. Cruvinel . A model for soil computed tomography based on volumetric reconstruction, Wiener filtering and parallel processing. Computers and Electronics in Agriculture 111 (2015) 151–163.

User Interface Image Reconstruction

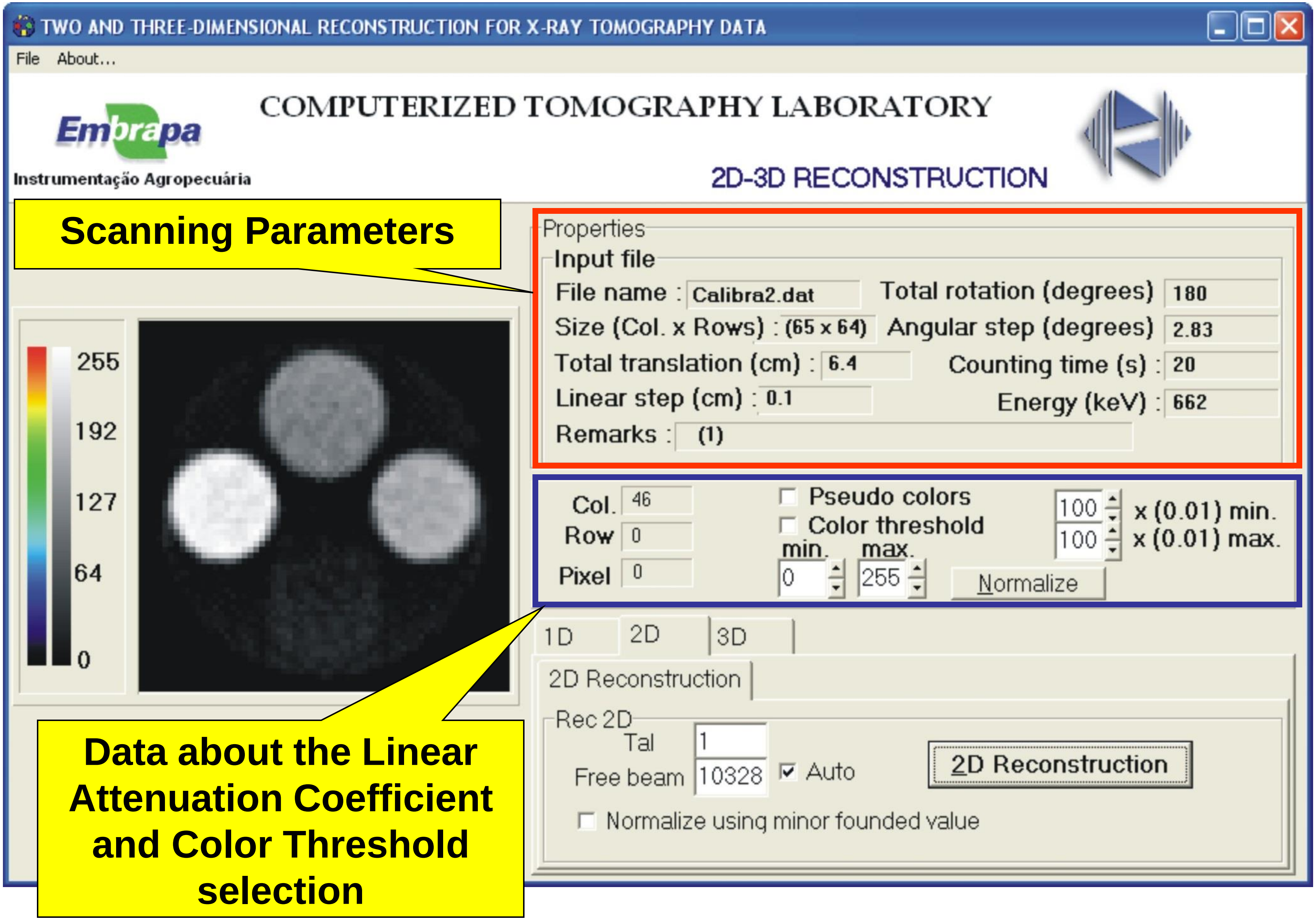

User Interface for 3D Image Visualization

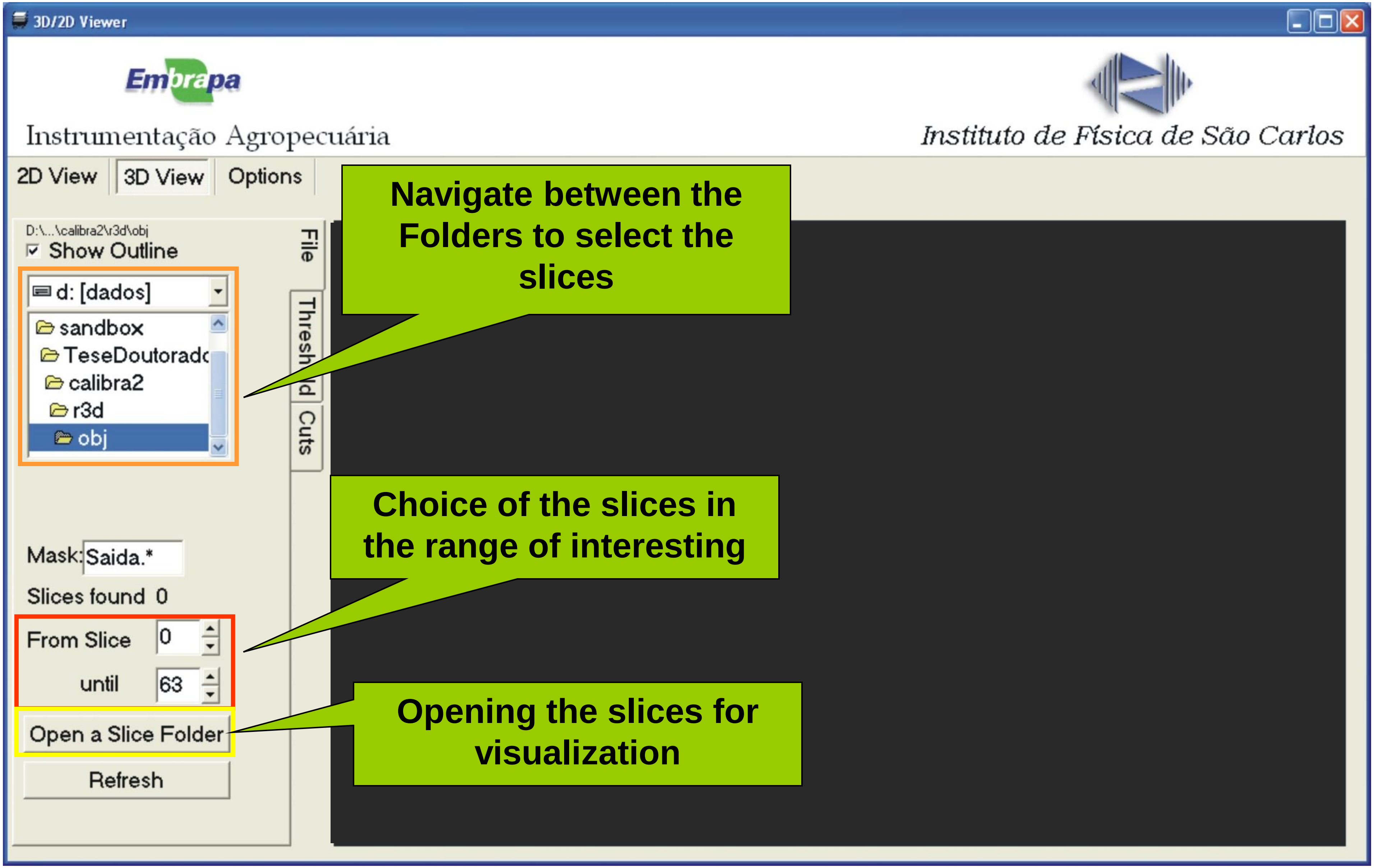

Agricultural Soil Sample Analysis

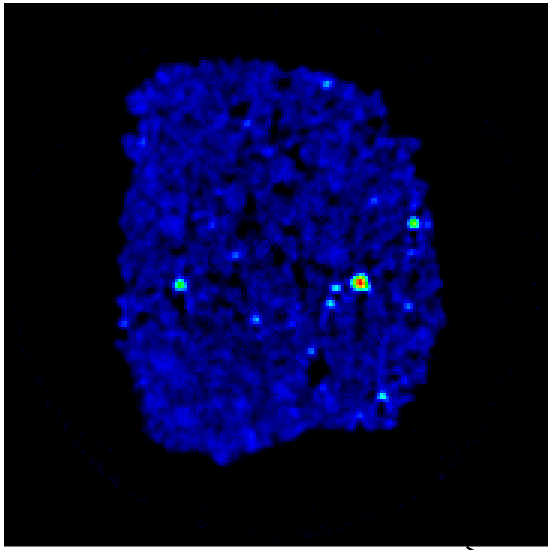

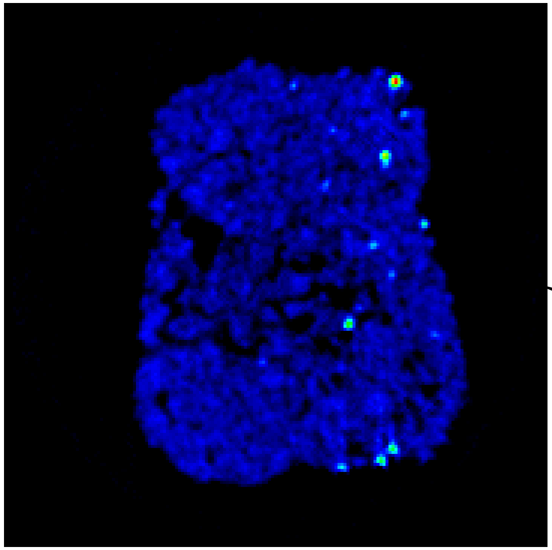

- To evaluate the potential of the 3D visualization model a study of a soil sample was carried out. These results demonstrate the potentials of the model as an analysis tool for application in research related to soil science;

Total translation	15.000 mm
Linear step	0.083mm
Angular step	1.000º
Window in time	4 seconds
Energy	58.5 keV

Depth of 88 mm

Depth of 158 mm

Agricultural Soil Sample Analysis

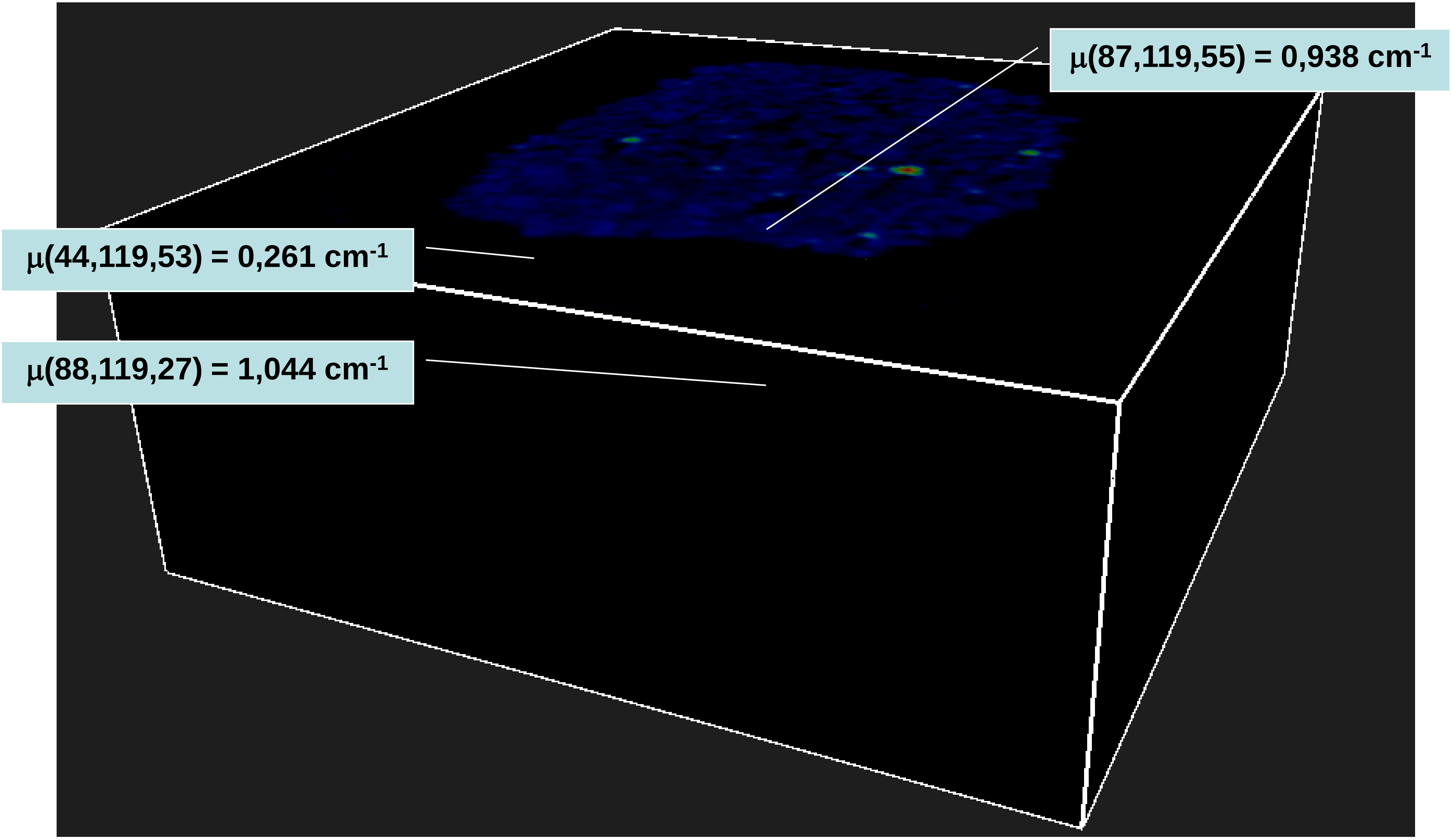

Soil Porosity Analysis

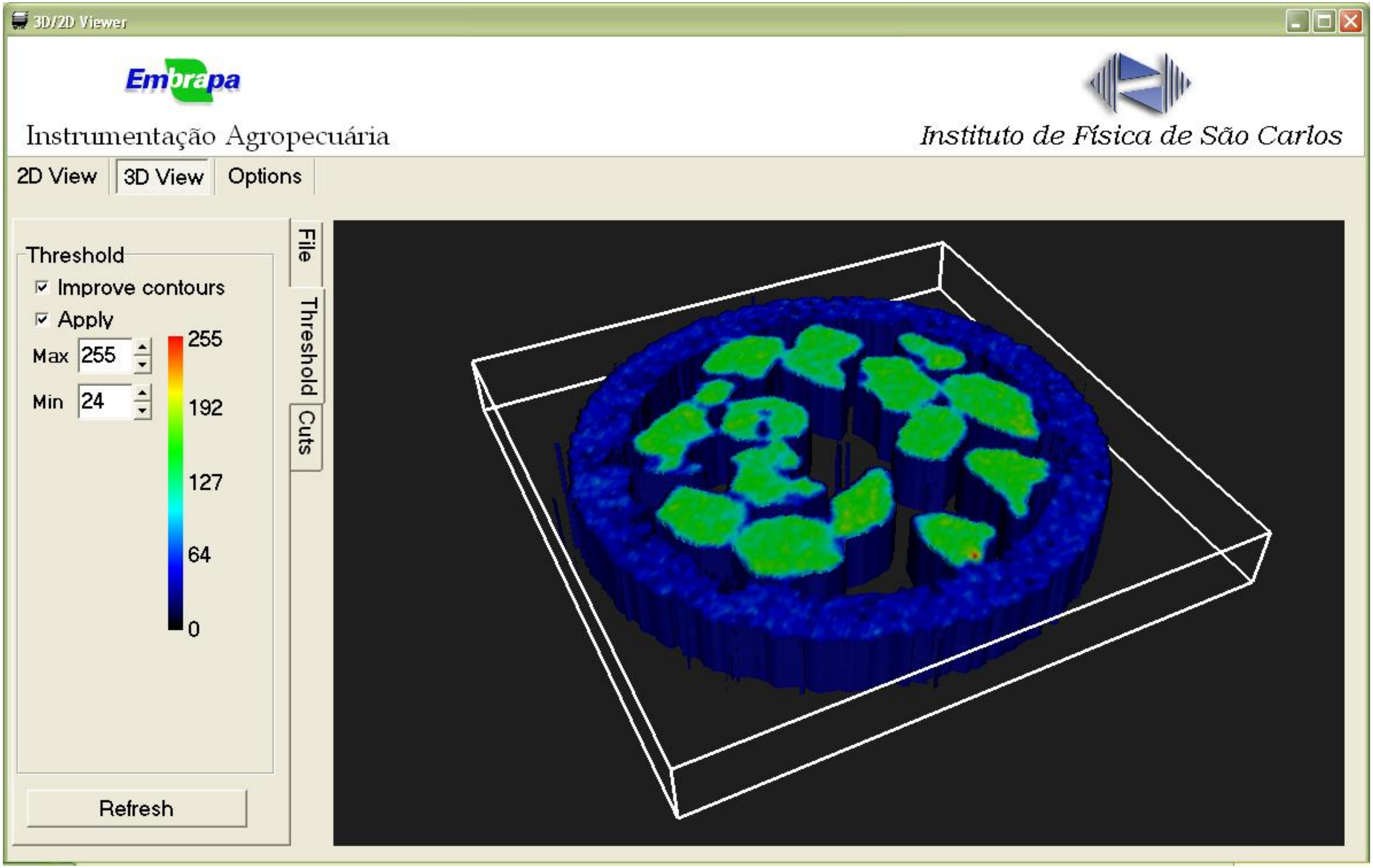

CT in Agriculture

SKYSCAN 1172: HIGH RESOLUTION DESK-TOP MICRO-CT

- DESCRIPTION
  - Fully distortion corrected 11Mp X-ray camera.
  - Up to 8000x8000 pixels in every slice.
  - Down to 0.5µm isotropic detail detectability.
  - Dynamically variable acquisition geometry for shortest scan at any magnification.
  - World's fastest hierarchical reconstruction (InstaRecon®) and GPU-accelerated FDK reconstruction.
  - Software for 2D/ 3D image analysis and realistic visualization by surface and volume rendering.

Bruker microCT

Applications: wood, paper, seeds (2) / SkyScan2211

<< other direct links here
<prev wood,paper,seeds next> <prev 2011 next> 2211specifications

Object: wood
Scanner: SkyScan2211
Image: three orthogonal virtual slices,400nm isotropic voxels

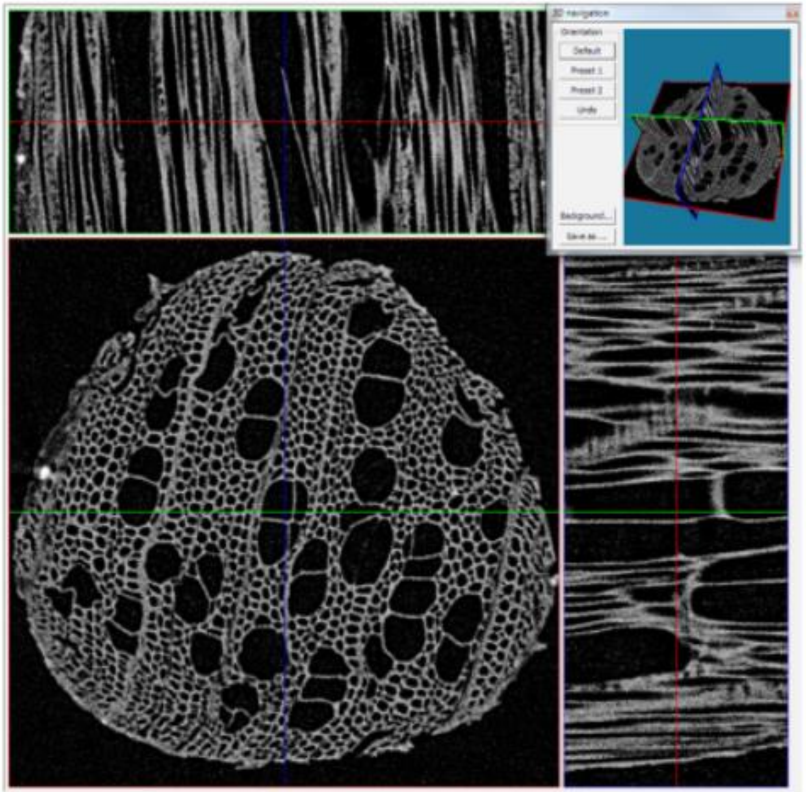

Image: 3D rendering of the sample internal microarchitecture (CTvox software)

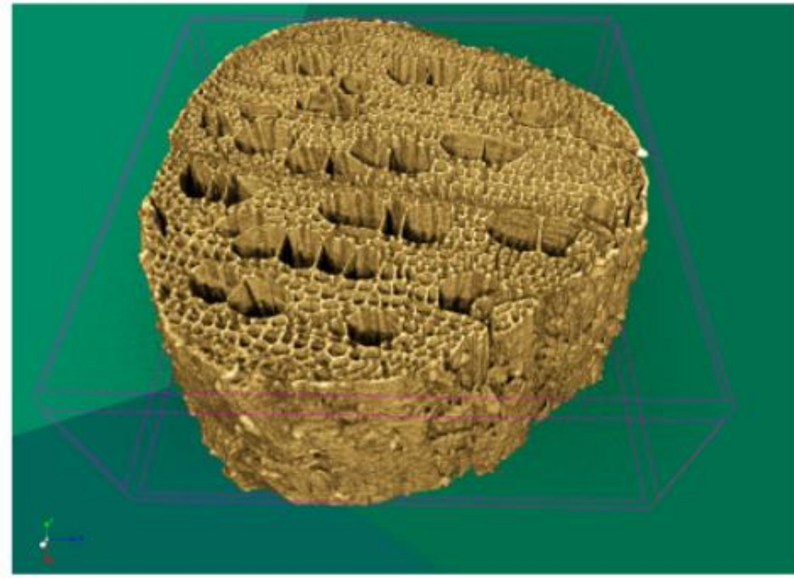

<prev wood,paper,seeds next> <prev 2011 next> 2211specifications

home

microtomography, nanotomography, micro-CT, nano-ct, microCT, nanoct, mikroct, mikro-ct, mikro-computertomographie, マイクロトモグラフィー, 高解像度,ナノ-CTの, 三次元, 非破壊検査, microtomographie, small animal imaging, non-invasive, non-destructive, NDT, NDE, 3D microscopy,tomography, microscopy, 3D, three-dimensional, medical imaging, small animals, volume rendering, volume visualization

Source: http://bruker-microct.com/applications/wood/wood002.htm

Acknowledgements

IARIA

Embrapa

Instrumentation

Thank You!